Table 2. The number and age of mice examined by sandwich enzyme-linked immunosorbent assay. Abbreviation: n = number of mice.

Age (months)	Tg2576/*TTR*$^{+/-}$ (n)	Tg2576/*TTR*$^{-/-}$ (n)
13	2	2
14	3	3
15	2	2
16	3	3
17	2	2
18	5	5
20	2	2
Total	19	19

Tg2576/*TTR*$^{-/-}$ mice relative to the age-matched Tg2576/*TTR*$^{+/-}$ mice ($P < 0.01$) (Figure 4C). On the other hand, there was no significant difference in the levels of Aβ42 in FA fraction between Tg2576/*TTR*$^{+/-}$ and Tg2576/*TTR*$^{-/-}$ mice (Figure 4D). The mean level of Aβ42 in FA fraction is much higher than that in SDS fraction. Thus, there was no significant difference in the sum of Aβ42 levels in both the fractions between aged Tg2576/*TTR*$^{+/-}$ and Tg2576/*TTR*$^{-/-}$ mice. Thus, TTR deficiency does not increase but rather decreases the level of Aβ40 in the brain of aged Tg2576 mice, a result, which is in good agreement with the immunohistochemistry data, suggesting that TTR increases the vascular Aβ burdens in the brain of aged mice (Figure 2).

Transthyretin deficiency does not affect the distribution and degree of tau phosphorylation in the brain of Tg2576 mice

In contrast to human AD, Tg2576 mice lack NFT, and develop the phosphorylated tau-immunoreactive aberrant structures that are exclusively associated with congophilic Aβ plaques (27, 48, 49). Stein *et al* reported that chronic infusion of an antibody against TTR into the hippocampus of Tg2576 led to an increase of tau phosphorylation within the CA1 neuronal field (42). To investigate whether or not TTR deficiency affected the distribution and degree of tau phosphorylation, the brain slices of 16–20-month-old Tg2576/*TTR*$^{+/-}$ and Tg2576/*TTR*$^{-/-}$ mice were stained with either

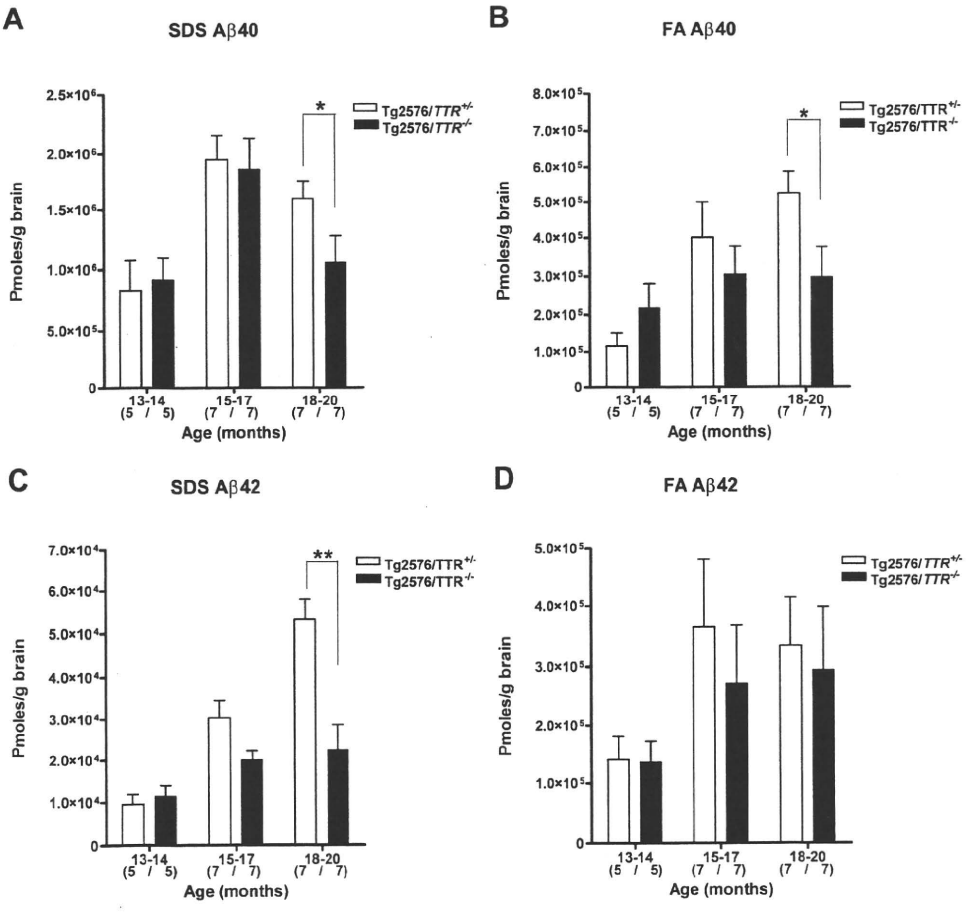

Figure 4. *The Aβ level in the brain of Tg2576/TTR*$^{+/-}$ *and Tg2576/TTR*$^{-/-}$ *mice.* The Aβ40 (**A,B**) and Aβ42 (**C,D**) in Tg2576/*TTR*$^{+/-}$ and Tg2576/*TTR*$^{-/-}$ brains were quantified by sandwich enzyme-linked immunosorbent assay. The samples were sequentially extracted in 2% sodium dodecylsulfate (SDS) (**A,C**) and 70% FA (**B,D**). All data are expressed as mean ± standard error of the mean. Numbers in parentheses denote numbers of mice examined. $^{*}P < 0.05$, $^{**}P < 0.01$. TTR = transthyretin.

AT8 or Thr231 antibody, as described under *Methods*. Both the antibodies reacted only with the punctate dystrophic neurites (DNs) within the Aβ plaques in hippocampus and cerebral cortex in both the mice (Figure 3B). The abundance of the DNs immunopositive with the antibodies in Tg2576/*TTR*$^{-/-}$ mice was much the same as that in Tg2576/*TTR*$^{+/-}$ mice (Figure 3B). No NFT was detected in any of the mice examined. Thus, TTR deficiency does not affect tau phosphorylation in the brain of Tg2576 mice.

No apoptotic cells are detected in the hippocampus of Tg2576/TTR$^{+/-}$ and Tg2576/TTR$^{-/-}$ mice

Tg2576 mice do not develop severe neuronal loss observed in AD (15). Stein and Johnson suggested that high level of TTR in the hippocampus of Tg2576 mice might protect the mice from severe neuronal loss (43). Furthermore, the same group reported that chronic infusion of an antibody against TTR into the hippocampus of Tg2576 mice led to an increase of neuronal loss and apoptosis within the CA1 neuronal field (42). To determine whether or not TTR deficiency induces apoptosis in the hippocampus of Tg2576 mice, the brain sections from 18–20-month-old Tg2576/*TTR*$^{+/-}$ and Tg2576/*TTR*$^{-/-}$ mice were subjected to TUNEL immunohistochemistry, as described under *Methods*. Apoptotic cells were never detected in the hippocampus or other parts of brain of any of the mice examined (Figure 3C). These results indicate that TTR deficiency does not induce apoptosis in the brain of Tg2576 mice.

DISCUSSION

To investigate the role of TTR in the Aβ deposition *in vivo*, we generated a mouse line carrying a null mutation at the endogenous *TTR* locus and the human mutant APP cDNA with the Swedish mutation (Tg2576/*TTR*$^{-/-}$ mouse) by crossing Tg2576 mice with TTR-deficient mice generated through gene targeting. We then asked whether Aβ deposition was accelerated in Tg2576/*TTR*$^{-/-}$ mice relative to the heterozygous mutant Tg2576 (Tg2576/*TTR*$^{+/-}$) mice. Contrary to our expectations, the degree of total Aβ deposition, tau phosphorylation and apoptosis in the brain was not increased by eliminating TTR in Tg2576 mice. Moreover, the degree of vascular Aβ burden in the aged Tg2576/*TTR*$^{-/-}$ mice was significantly reduced relative to the age-matched Tg2576/*TTR*$^{+/-}$ mice. Our experiments present, for the first time, compelling evidence that TTR does not suppress but rather accelerates vascular Aβ deposition in the mouse model of AD.

We confirmed that there was no significant difference in the onset, progression and distribution of total Aβ deposition between Tg2576/*TTR*$^{+/-}$ and Tg2576/*TTR*$^{-/-}$ mice up to age 17 months by immunohistochemistry (Figure 2A). However, total Aβ burden in 18–20-month-old Tg2576/*TTR*$^{-/-}$ mice was significantly reduced relative to the age-matched Tg2576/*TTR*$^{+/-}$ mice ($P < 0.05$) (Figure 2A). The result suggested that TTR does not suppress but rather accelerates Aβ deposition in the brain of Tg2576 mice. Although both Tg2576/*TTR*$^{+/-}$ and Tg2576/*TTR*$^{-/-}$ mice are smaller than non-transgenic littermates, both of them display no obvious phenotypic abnormalities, and their fertility is normal up to age 10 months. This observation is consistent with the immunohistochemistry data.

We then separately assessed vascular amyloid and plaque burdens in the brain of Tg2576/*TTR*$^{+/-}$ and Tg2576/*TTR*$^{-/-}$ mice. Although Aβ plaque burden was much the same between 7–20-month-old Tg2576/*TTR*$^{+/-}$ and Tg2576/*TTR*$^{-/-}$ mice (Figure 2C), vascular amyloid burden in the aged (18–20-month-old) Tg2576/*TTR*$^{-/-}$ mice was significantly reduced relative to the age-matched Tg2576/*TTR*$^{+/-}$ mice ($P < 0.05$) (Figure 2B). The quantification of Aβ40 and Aβ42 in the brain homogenates from Tg2576/*TTR*$^{+/-}$ and Tg2576/*TTR*$^{-/-}$ mice by sandwich ELISA demonstrated that TTR deficiency does not increase, but rather decreases the level of Aβ40 in the aged Tg2576 mice (Figure 4). Because the predominant Aβ peptide present in vascular amyloid deposits is reportedly Aβ40 (1, 7, 44), the result is also in good agreement with our immunohistochemistry data (Figure 2), suggesting that TTR increases the vascular Aβ burden in the brain of aged Tg2576 mice.

The reason why vascular amyloid burden is increased by TTR is not clear. Amyloid deposits of all types, including Aβ deposits, contain glycosaminoglycans (GAGs) and serum amyloid P component (SAP). A role for GAGs in amyloidosis is inferred from the observation that small molecules that interfere with GAG/amyloid interactions reduce murine experimental amyloid A (AA) amyloid progression (19). An amyloid-binding protein SAP protects amyloid fibrils from proteolysis *in vitro* (46), and the induction of AA amyloidosis is significantly retarded in the SAP-deficient mice relative to wild-type mice (4, 47). On the other hand, recent evidence indicates that Aβ is mainly cleared out of the brain to blood via transport through the blood-brain barrier, and via the interstitial fluid (ISF) bulk flow along periarterial drainage pathways into the CSF, and from there into the blood (26, 33, 52, 56). It is the CSF and perhaps the ISF and not the brain parenchyma (41) that is enriched in TTR. Thus we think it likely that when Aβ drains from the brain parenchyma along periarterial drainage pathways, it may come into contact with TTR which may protect Aβ deposits from proteolysis like GAG and SAP, thereby, slightly increases vascular amyloid burden over the ages.

Schwarzman *et al* reported that TTR in the CSF binds Aβ, and prevents Aβ fibril formation *in vitro*. They, however, also reported that apoE prevents Aβ fibril formation too (36, 37). It has been well established that apoE promotes assembly of Aβ fibril (23, 32). Thus, TTR may promote the fibrillization of Aβ too. Moreover, Holtzman *et al* found that a transgenic mouse model of AD on an apoE$^{-/-}$ background had significantly reduced Aβ deposition relative to the same mouse model expressing wild-type murine apoE (apoE$^{+/+}$), human apoE3 (apoE3$^{+/-}$) or human apoE4 (apoE4$^{+/-}$) (12). Therefore, TTR null Tg2576 (Tg2576/*TTR*$^{-/-}$) mice may represent mice that are unable to form Aβ fibrils, and the Aβ detected in the brain of the mice could be due in part to apoE.

Stein *et al* reported that chronic infusion of anti-TTR antibody into the hippocampus of Tg2576 mice increased Aβ burden, and led to tau hyperphosphorylation, neuronal loss and apoptosis in the CA1 neuronal field (42). These observations suggest the importance of TTR in inhibition of Aβ fibril formation and toxicity. However, contrary to these reports, our experiments suggested that TTR does not suppress but rather enhances Aβ deposition in Tg2576 mice. The reason for the discrepancy between data of other authors and our data is not clear. TTR is complexed with retinol-binding protein (RBP) and thyroid hormone *in vivo*. In the *in vitro* Aβ aggregation assay, however, recombinant TTR alone, not complexed with RBP or thyroid hormone, was used to examine its ability to inhibit Aβ fibril formation (36, 37). Association of TTR with RBP and thyroid hormone may affect its binding capacity

with Aβ *in vivo*. Tau phosphorylation and apoptosis were induced by Aβ in hippocampal cultures (42). Thus, as suggested by Stein *et al*, high intrahippocampal concentration of Aβ, induced temporarily by the disruption of TTR binding of Aβ by the antibody, might have caused localized neurodegeneration in the CA1 field. The neurodegeneration reportedly detected in the antibody-infused limited area of hippocampus of Tg2576 mice (42), however, was not detected in the entire brain of TTR-deficient Tg2576 mice.

Stein and Johnson reported that the lack of neurodegeneration was associated with increased level of TTR synthesized in the hippocampus of Tg2576 mice (43). However, Lazarov *et al* reported that the individual levels of TTR mRNA in the hippocampi of a transgenic mouse model of AD, which co-expresses familial AD-linked mutant APP, and presenilin 1 (PS1) cDNAs were considerably variable (20). Furthermore, it had been reported that choroid plexus is the sole site of TTR synthesis within the brain; in this regard, Sousa *et al* recently confirmed that TTR is not produced in the brain parenchyma of either wild-type or Tg2576 mice, using laser dissection microscopy (41). The finding suggests that contamination by choroid plexus might lead to misinterpretation of the role of TTR in Aβ deposition in the brain.

In the present study, we compared the onset and progression of Aβ pathology in TTR null Tg2576 (Tg2576/$TTR^{-/-}$) mice with those in heterozygous mutant Tg2576 mice (Tg2576$TTR^{+/-}$). Thus, one factor which causes the discrepancy between our data and other authors' data obtained by examining only Tg2576 mice homozygous for the wild-type *TTR* gene (Tg2576/$TTR^{+/+}$) for comparison might be the difference in the levels of TTR. However, the onset and progression of Aβ pathology in our Tg2576/$TTR^{+/-}$ mice are rather delayed than accelerated relative to those in Tg2576/$TTR^{+/+}$ mice previously reported by other authors (6, 18, 45, 55). Thus, the possibility that homozygous levels of TTR would be required to prevent Aβ pathology appears to be remote.

On the other hand, Nunes *et al* reported that peptidylglycine α-amidating monooxygenase, the rate-limiting enzyme in neuropeptide maturation, is over-expressed in the peripheral, and central nervous systems of $TTR^{-/-}$ mice that, consequently, display increased neuropeptide Y (NPY) levels relative to wild-type mice (28). NPY is known to be a substrate of neprilysin, which is an Aβ-degrading protease (50). Another Aβ-degrading enzyme, insulin-degrading enzyme (IDE) is also known as insulin and amylin protease (30, 50). Hyperinsulinaemia is known to increase the risk of developing AD. Thus, it is suggested that hyperinsulinaemia may elevate Aβ level through insulin's competition with Aβ for IDE (30). Analogous to the competition, the increase in NPY levels in $TTR^{-/-}$ mice might competitively reduce neprilysin clearance of Aβ. Thus, Tg2576/$TTR^{-/-}$ mice might display enhanced Aβ deposition relative to Tg2576/$TTR^{+/-}$ mice through NPY's competition with Aβ for neprilysin. Contrary to the expectation, Tg2576/$TTR^{-/-}$ mice display rather suppressed Aβ deposition relative to Tg2576/$TTR^{+/-}$ mice (Figures 2 and 4). The results say that TTR does not suppress but rather accelerates Aβ deposition in Tg2576 mice.

Contrary to our findings, Choi *et al* recently reported that in a different transgenic mouse model of AD heterozygous for the disrupted *TTR* gene ($TTR^{+/-}$), brain Aβ deposition is significantly accelerated relative to the age-matched model homozygous for the wild-type *TTR* gene ($TTR^{+/+}$) (8). Their observation, which suggests that TTR suppresses Aβ deposition, contradicts ours. It is important to note that there are several critical differences in the experimental designs which might have caused the contradiction between their data and ours: (i) the AD model mouse we examined (Tg2576) is distinct from that Choi *et al* examined. They used *ceAPPswe/PS1ΔE9* mice that harbor not only the human mutant APP cDNA with the double mutation K670N and M671L linked to a Swedish familial AD but also the human mutant PS1 cDNA with the exon 9 deletion linked to a familial AD (16, 21). In contrast to Tg2576 mice, their control singly transgenic mice that express the human mutant APP cDNA alone are free of brain Aβ deposits up to age 14 months and co-expression of human mutant APP, and PS1 accelerates the amyloid deposition (3, 21). Furthermore, comparative analysis of cortical gene expression patterns between Tg2576 mice homozygous for the PS1 knock-in mutation (Tg2576/$PS1^{264L/264L}$) and control Tg2576 mice heterozygous for the PS1 mutation (Tg2576/$PS1P^{264L/+}$) by DNA micro-array analysis revealed that the patterns are distinct, although there were some common regulated genes (54). All these observations suggest that the molecular pathogenesis of Aβ deposition in the two mouse models is different; (ii) the level of human variant APP in the brain of Tg2576 mice is more than fourfold higher than that of endogenous brain APP (14). On the other hand, although the level of human variant APP in the brain of *ceAPPswe/PS1ΔE9* mice is not described (8), variant PS1ΔE9 reportedly elevates Aβ42/Aβ40 ratio (3). Thus the contradiction between their results and ours might be caused by the significant difference in the levels of Aβ42 and/or Aβ40 between Tg2576 and *ceAPPswe/PS1ΔE9* mice; and (iii) Choi *et al* compared the degree of Aβ deposition between the brains of *ceAPPswe/PS1ΔE9* mice heterozygous for the disrupted *TTR* gene ($TTR^{+/-}$) and the mice homozygous for the wild-type *TTR* gene ($TTR^{+/+}$) (8), in contrast to the TTR null ($TTR^{-/-}$) and $TTR^{+/-}$ Tg2576 mice we examined for comparison. Thus in their study, in contrast to our study, the individual differences in the levels of brain TTR among the $TTR^{+/-}$ and control $TTR^{+/+}$ mice should critically affect the results, and hence, the elucidation of the relationship between TTR and Aβ deposition. They described that the levels of immunoreactive TTR in the extracts from the brains of *ceAPPswe/PS1ΔE9/*$TTR^{+/-}$ mice are clearly lower relative to the age-matched *ceAPPswe/PS1ΔE9/*$TTR^{+/+}$ mice at all ages examined (8). However, the report is lacking in important details about the levels of TTR in the individual animals that would make the data more compelling. For example, given only the pictorial data with sample number of 1, it is not clear that the differences in the brain levels of TTR between *ceAPPswe/PS1ΔE9/*$TTR^{+/+}$ and *ceAPPswe/PS1ΔE9/*$TTR^{+/-}$ mice are really significant. On the other hand, it is possible that TTR, as a peripheral Aβ binding protein, may have the ability to act as a peripheral Aβ 'sink'; whereby, it pulls Aβ from the brain into the periphery, hence decreasing the amount of Aβ in the brain (26, 33, 52, 56). Thus, if we had examined Tg2576$TTR^{+/+}$ mice, we, too, might have detected a decrease in Aβ deposition as Choi *et al* did.

All the above differences may cause the contradiction between their data and ours. Moreover, they described that the levels of brain TTR were significantly lower in human AD patients compared with age-matched controls and negatively correlated with the abundance of amyloid plaques. However, the references they cited didn't refer to the brain TTR levels but to the CSF TTR levels in the patients (8) and, to our knowledge, the comparison of the brain TTR levels between AD patients and control disease-free individuals has not yet been reported.

In conclusion, our results indicated, for the first time, TTR does not suppress but accelerates vascular Aβ burden in the brain of Tg2576 mice. However, the mechanism(s) by which TTR affects the Aβ deposition *in vivo* are not yet elucidated. Taken together with the Choi et al's contradictory finding (8), our finding suggests that the role of TTR in the pathogenesis of AD remains to be understood.

ACKNOWLEDGMENTS

The authors would like to thank Drs. K. H. Ashe and Takaomi C. Saido for provision of Tg2576 mice and Ab9204 antibody, respectively. This work was supported by grants from the Ministry of Education, Culture, Sports, Science and Technology, Japan: Grants-in-aids for Scientific Research (18390098; to SM); and by grants to the Amyloidosis Research Committee for the Research on Intractable Diseases from the Ministry of Health, Labour and Welfare, Japan (to MS & SM).

REFERENCES

1. Alonzo NC, Hyman BT, Rebeck GW, Greenberg SM (1998) Progression of cerebral amyloid angiopathy: accumulation of amyloid-beta40 in affected vessels. *J Neuropathol Exp Neurol* **57**:353–359.
2. Biroccio A, Del Boccio P, Panella M, Bernardini S, Di Ilio C, Gambi D *et al* (2006) Differential post-translational modifications of transthyretin in Alzheimer's disease: a study of the cerebral spinal fluid. *Proteomics* **6**:2305–2313.
3. Borchelt DR, Ratovitski T, van Lare J, Lee MK, Gonzales V, Jenkins NA *et al* (1997) Accelerated amyloid deposition in the brains of transgenic mice coexpressing mutant presenilin 1 and amyloid precursor proteins. *Neuron* **19**:939–945.
4. Botto M, Hawkins PN, Bickerstaff MC, Herbert J, Bygrave AE, McBride A *et al* (1997) Amyloid deposition is delayed in mice with targeted deletion of the serum amyloid P component gene. *Nat Med* **3**:855–859.
5. Braak H, Braak E (1991) Neuropathological stageing of Alzheimer-related changes. *Acta Neuropathol (Berl)* **82**: 239–259.
6. Carro E, Trejo JL, Gomez-Isla T, LeRoith D, Torres-Aleman I (2002) Serum insulin-like growth factor I regulates brain amyloid-beta levels. *Nat Med* **8**:1390–1397.
7. Castano EM, Prelli F, Soto C, Beavis R, Matsubara E, Shoji M, Frangione B (1996) The length of amyloid-beta in hereditary cerebral hemorrhage with amyloidosis, Dutch type. Implications for the role of amyloid-beta 1-42 in Alzheimer's disease. *J Biol Chem* **271**:32185–32191.
8. Choi SH, Leight SN, Lee VM, Li T, Wong PC, Johnson JA, Saraiva MJ, Sisodia SS (2007) Accelerated Abeta deposition in APPswe/PS1deltaE9 mice with hemizygous deletions of TTR (transthyretin). *J Neurosci* **27**:7006–7010.
9. Episkopou V, Maeda S, Nishiguchi S, Shimada K, Gaitanaris GA, Gottesman ME, Robertson EJ (1993) Disruption of the transthyretin gene results in mice with depressed levels of plasma retinol and thyroid hormone. *Proc Natl Acad Sci USA* **90**:2375–2379.
10. Giunta S, Valli MB, Galeazzi R, Fattoretti P, Corder EH, Galeazzi L (2005) Transthyretin inhibition of amyloid beta aggregation and toxicity. *Clin Biochem* **38**:1112–1119.
11. Hardy J, Selkoe DJ (2002) The amyloid hypothesis of Alzheimer's disease: progress and problems on the road to therapeutics. *Science* **297**:353–356.
12. Holtzman DM, Bales KR, Tenkova T, Fagan AM, Parsadanian M, Sartorius LJ *et al* (2000) Apolipoprotein E isoform-dependent amyloid deposition and neuritic degeneration in a mouse model of Alzheimer's disease. *Proc Natl Acad Sci USA* **97**:2892–2897.
13. Hsiao K, Chapman P, Nilsen S, Eckman C, Harigaya Y, Younkin S *et al* (1996) Correlative memory deficits, Abeta elevation, and amyloid plaques in transgenic mice. *Science* **274**:99–102.
14. Hsiao KK, Borchelt DR, Olson K, Johannsdottir R, Kitt C, Yunis W *et al* (1995) Age-related CNS disorder and early death in transgenic FVB/N mice overexpressing Alzheimer amyloid precursor proteins. *Neuron* **15**:1203–1218.
15. Irizarry MC, McNamara M, Fedorchak K, Hsiao K, Hyman BT (1997) APPSw transgenic mice develop age-related A beta deposits and neuropil abnormalities, but no neuronal loss in CA1. *J Neuropathol Exp Neurol* **56**:965–973.
16. Jankowsky JL, Slunt HH, Ratovitski T, Jenkins NA, Copeland NG, Borchelt DR (2001) Co-expression of multiple transgenes in mouse CNS: a comparison of strategies. *Biomol Eng* **17**:157–165.
17. Joachim CL, Duffy LK, Morris JH, Selkoe DJ (1988) Protein chemical and immunocytochemical studies of meningovascular beta-amyloid protein in Alzheimer's disease and normal aging. *Brain Res* **474**:100–111.
18. Kawarabayashi T, Younkin LH, Saido TC, Shoji M, Ashe KH, Younkin SG (2001) Age-dependent changes in brain, CSF, and plasma amyloid (beta) protein in the Tg2576 transgenic mouse model of Alzheimer's disease. *J Neurosci* **21**:372–381.
19. Kisilevsky R, Lemieux LJ, Fraser PE, Kong X, Hultin PG, Szarek WA (1995) Arresting amyloidosis in vivo using small-molecule anionic sulphonates or sulphates: implications for Alzheimer's disease. *Nat Med* **1**:143–148.
20. Lazarov O, Lee M, Peterson DA, Sisodia SS (2002) Evidence that synaptically released beta-amyloid accumulates as extracellular deposits in the hippocampus of transgenic mice. *J Neurosci* **22**:9785–9793.
21. Lazarov O, Robinson J, Tang YP, Hairston IS, Korade-Mirnics Z, Lee VM *et al* (2005) Environmental enrichment reduces Abeta levels and amyloid deposition in transgenic mice. *Cell* **120**:701–713.
22. Link CD (1995) Expression of human beta-amyloid peptide in transgenic Caenorhabditis elegans. *Proc Natl Acad Sci USA* **92**:9368–9372.
23. Ma J, Yee A, Brewer HB, Das S, Potter H (1994) Amyloid-associated proteins α_1-antichymotrypsin and apolipoprotein E promote assembly of Alzheimer β-protein into filaments. *Nature* **372**:92–94.
24. Matsubara E, Bryant-Thomas T, Pacheco Quinto J, Henry TL, Poeggeler B, Herbert D *et al* (2003) Melatonin increases survival and inhibits oxidative and amyloid pathology in a transgenic model of Alzheimer's disease. *J Neurochem* **85**:1101–1108.
25. Matsubara E, Ghiso J, Frangione B, Amari M, Tomidokoro Y, Ikeda Y *et al* (1999) Lipoprotein-free amyloidogenic peptides in plasma are elevated in patients with sporadic Alzheimer's disease and Down's syndrome. *Ann Neurol* **45**:537–541.
26. Matsuoka Y, Saito M, LaFrancois J, Saito M, Gaynor K, Olm V *et al* (2003) Novel therapeutic approach for the treatment of Alzheimer's disease by peripheral administration of agents with an affinity to beta-amyloid. *J Neurosci* **23**:29–33.
27. Noda-Saita K, Terai K, Iwai A, Tsukamoto M, Shitaka Y, Kawabata S *et al* (2004) Exclusive association and simultaneous appearance of congophilic plaques and AT8-positive dystrophic neurites in Tg2576 mice suggest a mechanism of senile plaque formation and progression of neuritic dystrophy in Alzheimer's disease. *Acta Neuropathol (Berl)* **108**:435–442.
28. Nunes AF, Saraiva MJ, Sousa MM (2006) Transthyretin knockouts are a new mouse model for increased neuropeptide Y. *Faseb J* **20**:166–168.

29. Prelli F, Castano E, Glenner GG, Frangione B (1988) Differences between vascular and plaque core amyloid in Alzheimer's disease. *J Neurochem* **51**:648–651.
30. Qiu WQ, Folstein MF (2006) Insulin, insulin-degrading enzyme and amyloid-beta peptide in Alzheimer's disease: review and hypothesis. *Neurobiol Aging* **27**:190–198.
31. Rensink AA, de Waal RM, Kremer B, Verbeek MM (2003) Pathogenesis of cerebral amyloid angiopathy. *Brain Res Brain Res Rev* **43**:207–223.
32. Sadowski MJ, Pankiewicz J, Scholtzova H, Mehta PD, Prelli F, Quartermain D, Wisniewski T (2006) Blocking the apolipoprotein E/amyloid-beta interaction as a potential therapeutic approach for Alzheimer's disease. *Proc Natl Acad Sci USA* **103**:18787–18792.
33. Sagare A, Deane R, Bell RD, Johnson B, Hamm K, Pendu R *et al* (2007) Clearance of amyloid-β by circulating lipoprotein receptors. *Nat Med* **13**:1029–1031.
34. Saido TC, Iwatsubo T, Mann DM, Shimada H, Ihara Y, Kawashima S (1995) Dominant and differential deposition of distinct beta-amyloid peptide species, a beta N3(pE), in senile plaques. *Neuron* **14**:457–466.
35. Sasaki A, Shoji M, Harigaya Y, Kawarabayashi T, Ikeda M, Naito M *et al* (2002) Amyloid cored plaques in Tg2576 transgenic mice are characterized by giant plaques, slightly activated microglia, and the lack of paired helical filament-typed, dystrophic neurites. *Virchows Arch* **441**:358–367.
36. Schwarzman AL, Goldgaber D (1996) Interaction of transthyretin with amyloid beta-protein: binding and inhibition of amyloid formation. *Ciba Found Symp* **199**:146–160.discussion 60–64.
37. Schwarzman AL, Gregori L, Vitek MP, Lyubski S, Strittmatter WJ, Enghilde JJ *et al* (1994) Transthyretin sequesters amyloid beta protein and prevents amyloid formation. *Proc Natl Acad Sci USA* **91**:8368–8372.
38. Serot JM, Christmann D, Dubost T, Couturier M (1997) Cerebrospinal fluid transthyretin: aging and late onset Alzheimer's disease. *J Neurol Neurosurg Psychiatry* **63**:506–508.
39. Seubert P, Vigo-Pelfrey C, Esch F, Lee M, Dovey H, Davis D *et al* (1992) Isolation and quantification of soluble Alzheimer's beta-peptide from biological fluids. *Nature* **359**:325–327.
40. Shoji M, Golde TE, Ghiso J, Cheung TT, Estus S, Shaffer LM *et al* (1992) Production of the Alzheimer amyloid beta protein by normal proteolytic processing. *Science* **258**:126–129.
41. Sousa JC, Cardoso I, Marques F, Saraiva MJ, Palha JA (2007) Transthyretin and Alzheimer's disease: where in the brain? *Neurobiol Aging* **28**:713–718.
42. Stein TD, Anders NJ, DeCarli C, Chan SL, Mattson MP, Johnson JA (2004) Neutralization of transthyretin reverses the neuroprotective effects of secreted amyloid precursor protein (APP) in APPSW mice resulting in tau phosphorylation and loss of hippocampal neurons: support for the amyloid hypothesis. *J Neurosci* **24**:7707–7717.
43. Stein TD, Johnson JA (2002) Lack of neurodegeneration in transgenic mice overexpressing mutant amyloid precursor protein is associated with increased levels of transthyretin and the activation of cell survival pathways. *J Neurosci* **22**:7380–7388.
44. Suzuki N, Iwatsubo T, Odaka A, Ishibashi Y, Kitada C, Ihara Y (1994) High tissue content of soluble beta 1-40 is linked to cerebral amyloid angiopathy. *Am J Pathol* **145**:452–460.
45. Takeuchi A, Irizarry MC, Duff K, Saido TC, Hsiao Ashe K, Hasegawa M *et al* (2000) Age-related amyloid beta deposition in transgenic mice overexpressing both Alzheimer mutant presenilin 1 and amyloid beta precursor protein Swedish mutant is not associated with global neuronal loss. *Am J Pathol* **157**:331–339.
46. Tennent GA, Lovat LB, Pepys MB (1995) Serum amyloid P component prevents proteolysis of the amyloid fibrils of Alzheimer disease and systemic amyloidosis. *Proc Natl Acad Sci USA* **92**:4299–4303.
47. Togashi S, Lim SK, Kawano H, Ito S, Ishihara T, Okada Y *et al* (1997) Serum amyloid P component enhances induction of murine amyloidosis. *Lab Invest* **77**:525–531.
48. Tomidokoro Y, Harigaya Y, Matsubara E, Ikeda M, Kawarabayashi T, Shirao T *et al* (2001) Brain Abeta amyloidosis in APPsw mice induces accumulation of presenilin-1 and tau. *J Pathol* **194**:500–506.
49. Tomidokoro Y, Ishiguro K, Harigaya Y, Matsubara E, Ikeda M, Park JM *et al* (2001) Abeta amyloidosis induces the initial stage of tau accumulation in APP (SW) mice. *Neurosci Lett* **299**:169–172.
50. Wang DS, Dickson DW, Malter JS (2006) beta-Amyloid degradation and Alzheimer's disease. *J Biomed Biotechnol* **2006**:58406.
51. Wei L, Kawano H, Fu X, Cui D, Ito S, Yamamura K *et al* (2004) Deposition of transthyretin amyloid is not accelerated by the same amyloid in vivo. *Amyloid* **11**:113–120.
52. Weller RO, Cohen NR, Nicoll JA (2004) Cerebrovascular disease and the pathophysiology of Alzheimer's disease. Implications for therapy. *Panminerva Med* **46**:239–251.
53. Westerman MA, Cooper-Blacketer D, Mariash A, Kotilinek L, Kawarabayashi T, Younkin LH *et al* (2002) The relationship between Abeta and memory in the Tg2576 mouse model of Alzheimer's disease. *J Neurosci* **22**:1858–1867.
54. Wu ZL, Ciallella JR, Flood DG, O'Kane TM, Bozyczko-Coyne D, Savage MJ (2006) Comparative analysis of cortical gene expression in mouse models of Alzheimer's disease. *Neurobiol Aging* **27**:377–386.
55. Yang F, Lim GP, Begum AN, Ubeda OJ, Simmons MR, Ambegaokar SS *et al* (2005) Curcumin inhibits formation of amyloid beta oligomers and fibrils, binds plaques, and reduces amyloid in vivo. *J Biol Chem* **280**:5892–5901.
56. Zlokovic BV (2004) Clearing amyloid through the blood-brain barrier. *J Neurochem* **89**:807–811.

BRAIN RESEARCH 1250 (2009) 232–241

available at www.sciencedirect.com

ScienceDirect

www.elsevier.com/locate/brainres

BRAIN RESEARCH

Research Report

Motor impairment and aberrant production of neurochemicals in human α-synuclein A30P+A53T transgenic mice with α-synuclein pathology☆

Masaki Ikeda[a], *Takeshi Kawarabayashi*[b], *Yasuo Harigaya*[d], *Atsushi Sasaki*[c], *Shuichi Yamada*[g], *Etsuro Matsubara*[e], *Tetsuro Murakami*[f], *Yuya Tanaka*[f], *Tomoko Kurata*[f], *Xu Wuhua*[f], *Kenji Ueda*[h], *Hisashi Kuribara*[i], *Yasushi Ikarashi*[j], *Yoichi Nakazato*[c], *Koichi Okamoto*[a], *Koji Abe*[f], *Mikio Shoji*[b,*]

[a]*Department of Neurology, Gunma University Graduate School of Medicine, Maebashi, Japan*
[b]*Department of Neurology, Hirosaki University School of Medicine, Hirosaki, Japan*
[c]*Department of Human Pathology, Gunma University Graduate School of Medicine, Maebashi, Japan*
[d]*Department of Neurology, Maebashi Red Cross Hospital, Maebashi, Gunma, Japan*
[e]*Department of Alzheimer's Disease Research, National Institute for Longevity Sciences, Obu, Japan*
[f]*Department of Neurology, Neuroscience, Biophysiological Science, Okayama University Graduate School of Medicine and Dentistry, Okayama, Japan*
[g]*Immuno-Biological Laboratories Co., Ltd., Mikasa, Hokkaidio, Japan*
[h]*Department of Neural Plasticity, Tokyo Institute of Psychiatry, Setagaya-ku, Tokyo, Japan*
[i]*Tokyo University of Social Welfare, Isesaki, Japan*
[j]*R and D Division, Tsumura and Co., Ltd, Inashiki, Japan*

ARTICLE INFO

Article history:
Accepted 6 October 2008
Available online 1 November 2008

Keywords:
α-synuclein
Mutation
Transgenic mouse
Parkinson's disease
Neurochemical

ABSTRACT

Missense point mutations, duplication and triplication in the α-synuclein (αSYN) gene have been identified in familial Parkinson's disease (PD). Familial and sporadic PD show common pathological features of αSYN pathologies, e.g., Lewy bodies (LBs) and Lewy neurites (LNs), and a loss of dopaminergic neurons in the substantia nigra that leads to motor disturbances. To elucidate the mechanism of αSYN pathologies, we generated TgαSYN transgenic mice overexpressing human αSYN with double mutations in A30P and A53T. Human αSYN accumulated widely in neurons, processes and aberrant neuronal inclusion bodies. Sarcosyl-insoluble αSYN, as well as phosphorylated, ubiquitinated and nitrated αSYN, was accumulated in the brains. Significantly decreased levels of dopamine (DA) were recognized in the striatum. Motor impairment was revealed in a rotarod test. Thus, TgαSYN is a useful model for analyzing the pathological cascade from aggregated αSYN to motor disturbance, and may be useful for drug trials.

☆ Grant numbers and sources of supports: Supported by **Grant-in-Aid for** Grants-in-Aid for Primary Amyloidosis Research Committee (M. S.), from the Ministry of Health, Labor and Welfare of Japan and by Grants-in-Aid for Scientific Research (B) (M.S.: 19390233, K.A.: 18390257), (C) (M.I.: 19590980, T.K.: 19590976, A.S.: 18500276, E.M.: 18590968), from the Ministry of Education, Culture, Sports, Science and Technology, Japan.

* *Corresponding author.* Fax: +81 172 39 5143.
E-mail address: mshoji@hirosaki-u.ac.jp (M. Shoji).

0006-8993/$ – see front matter © 2008 Published by Elsevier B.V.
doi:10.1016/j.brainres.2008.10.011

1. Introduction

αSYN was originally isolated from senile plaques in Alzheimer's disease as a protein of 35 highly hydrophobic amino acid metabolites, known as the non-amyloid component (NAC), derived from a 140 amino-acid precursor encoded by a gene on chromosome 4 (Ueda et al., 1992; Chen et al., 1995), which has homology to rat and Torpedo αSYN and songbird synelfin (George et al., 1995). αSYN is highly abundant in presynaptic terminals (Iwai et al., 1995) and has potential roles in synaptic function and neural plasticity (George et al., 1995; Clayton and George, 1998).αSYN binds to phospholipid vesicles and inhibits PLD2, a regulator of vesicle membrane budding (Liscovitch et al., 2000; Lotharius and Brundin, 2000; Payton et al., 2000), and also plays modulatory roles in the release of dopamine vesicles (Abeliovich et al., 2000).

A few cases of familial Parkinson's disease (FPD) have been linked to missense point mutations in αSYN with A53T (Polymeropoulos et al., 1997), A30P (Kruger et al., 1998) and E46K (PARK1) (Zarranz et al., 2004). Soon after the first A53T missense mutation of αSYN was discovered, the main component of Lewy bodies (LBs) was identified as insoluble aggregates of αSYN (Baba et al., 1998). αSYN and phosphorylated-Ser129 αSYN accumulated in LBs and Lewy neurites (LNs) in PD and Dementia with Lewy bodies (DLB) (Fujiwara et al., 2002; Hasegawa et al., 2002). Then, a second causative gene known as *parkin* (Kitada et al., 1998) was found in familial autosomal recessive juvenile Parkinson's disease (PARK2). *Parkin* ubiquitinates αSYN normally and this process is aberrantly altered in PD (Shimura et al., 2001). Acceleration of oligomerization or protofibrillization is a common property of mutant αSYN (Conway et al., 2001; Choi et al., 2004). Recently, triplication of the αSYN locus (PARK4) was identified in an "Iowanian kindred" with autosomal dominant Lewy body disease (Singleton et al., 2002). Subsequently, duplication of the αSYN gene locus was also reported as a cause of familial PD (Chartier-Harlin et al., 2004). These findings suggest that overexpression of wild type αSYN also leads to facilitation of insoluble aggregation of αSYN. α-synucleinopathy is a disease entity which shares common pathological accumulation of insoluble aggregates of αSYN in the neurons and processes of PD, DLB, Hallervorden–Spatz disease, pure autonomic failure and in the glial cells of multiple system atrophy (MSA) (Goedert, 2000; Hardy and Gwinn-Hardy, 1998; Spillantini et al., 1997; Tu et al., 1998; Galvin et al., 2000; Shoji et al., 2000; Arai et al., 2000).

To elucidate the pathological mechanism of LBs and LNs associated with the decrease in dopamine (DA) production, it is necessary to investigate the aberrant mechanism of mutant αSYN, which is an essential molecule consisting of LBs and LNs (Baba et al., 1998). Here, we generated transgenic (Tg) mice expressing human mutant αSYN A30P+A53T under a human Thy-1 promoter, named as TgαSYN. Overexpression of double mutant human αSYN was expected to lead to further synergistic effects and induce severe α-synucleinopathies and neurodegeneration (Citron et al., 1998; Chishti et al., 2001). TgαSYN showed significant motor impairment in rotarod test, accumulation of insoluble αSYN, aberrant inclusions and decreased dopamine levels. These findings indicate that TgαSYN is a useful animal model to investigate the crucial pathogenesis of α-synucleinopathies, and it may help to develop therapeutic agents.

2. Results

2.1. *Expression of αSYN in transgenic mice and analyses of RT-PCR*

We used the transgene construct hThy1-αSYN A30P+A53T to generate transgenic (Tg) mice, TgαSYN (Fig. 1a). PCR analysis of tail-derived DNA revealed 18 positive Tg mice for human αSYN and EGFP among 129 F0 mice. Five of the 18 Tg mice showed the strongest green fluorescence under irradiation at 365 nm ultraviolet (Fig. 1b). These selected independent lines (#8707, #8713, #8718, #8812, #8819) were mated with BDF1 mice and raised for examination. The following Tg mice were analyzed: 18 positive Tg progenies, 60 F1 Tg (#8707: 2, #8713: 31, #8718: 5, #8812: 10, #8819: 12) and 135 F2 Tg (#8707: 0, #8713: 101, #8718: 2, #8812: 29, #8819: 3). The mRNA expressions of human αSYN A30P+A53T and EGFP in TgαSYN brains were confirmed by RT-PCR, showing the same expression levels of human αSYN A30P+A53T and EGFP at three, eight and 17 months old, respectively (Figs. 1c and d). Western blot using LB509 recognized a 16 kD band corresponding to human αSYN only in Tg mice. AB5038 recognized a 16 kD band corresponding to both human and mouse αSYN. The expression level of human αSYN was 130% of that of endogenous mouse αSYN (Fig. 1e).

2.2. *Histological studies*

Immunocytochemistry of sagittal sections of a seven-month-old #8707 TgαSYN brain by LB509 revealed extensive human αSYN immunostaining in the brainstem, hippocampus, thalamus, cerebral cortex and cerebellum (Fig. 2a, arrow indicates the substantia nigra), but no staining in the non-Tg mouse (Fig. 2b). The TgαSYN brain showed atrophy of the cerebral cortex and cerebellum (Fig. 2a). The HE stain showed eosinophilic inclusion bodies and vacuoles in the cytoplasm of neurons in the substantia nigra (Fig. 2c, arrow), and in the dentate nucleus of TgαSYN (Fig. 2h, arrow). These cytoplasmic inclusions were stained with human-αSYN specific antibody, LB509 (Fig. 2d, arrow, and Fig. 2i, arrow), and anti-αSYN antibody, 42/α-Synuclein (Fig. 2j, arrows). Nitrated α/β synuclein was also stained in the cytoplasmic inclusions (Fig. 2e, arrow,). Ubiquitin-positive inclusions were observed in neurons at brainstem (Fig. 2f, arrow), and dystrophic neurites in the dentate nucleus of TgαSYN (Fig. 2g). Staining of phosphorylated synuclein showed diffuse staining in somatodendrites of TgαSYN neurons (Fig. 2k). Gallyas–Braak staining revealed dystrophic neurites in the dentate nucleus of TgαSYN (Fig. 2l) in ubiquitin-positive structures in the same region (Fig. 2g). Anti-tyrosine hydroxylase (TH) immuno-positive neurons in the locus ceruleus showed weak immunostaining intensity in TgαSYN (Fig. 2m), compared with those of non-Tg mice brains (Fig. 2n). The intensity of substance P immunopositive synapses in the striata of TgαSYN brains (Fig. 2o) was weaker than that of non-Tg mice brains (Fig. 2p). Severe astrocytosis

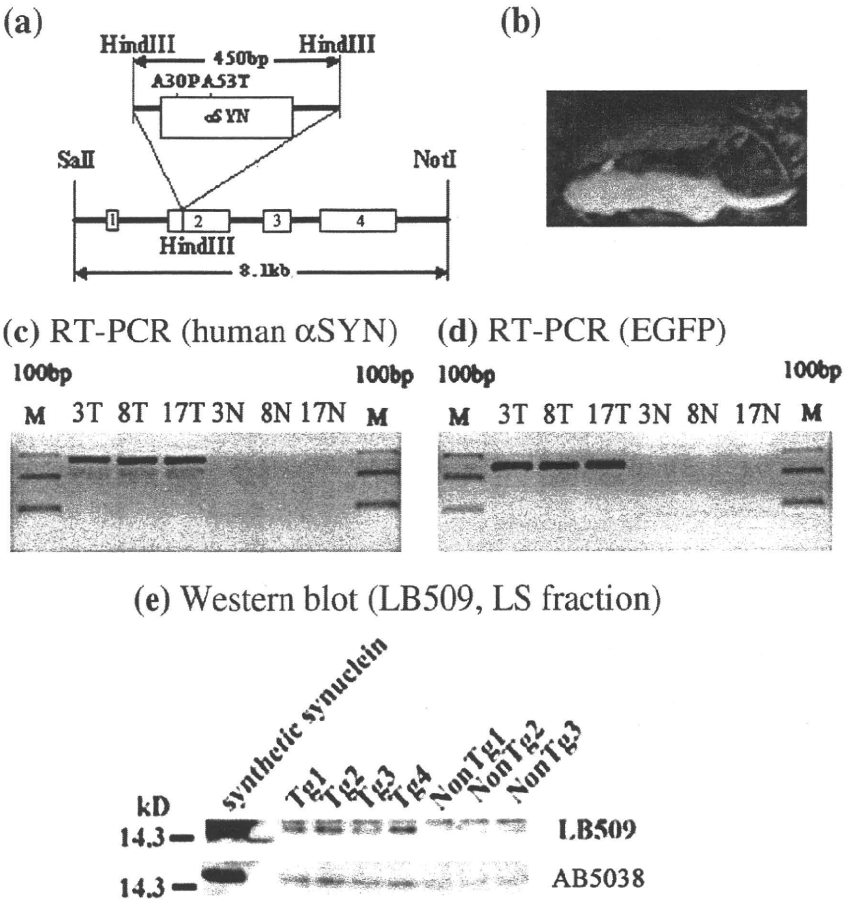

Fig. 1 – The mutant αSYN A30P+A53T construct and the expression of EGFP. (a) The structure of the construct: hThy1-αSYN A30P+A53T. (b) TgαSYN (#8713) showed fluorescence by EGFP (enhanced green fluorescence protein) under 365 nm long wave UV (EGFP-negative non-Tg mouse in the upper location, EGFP-positive Tg mouse in the lower location). (c) Analyses of RT-PCR transcripts: Human αSYN mRNA transcripts (exons 2–4) were detected as 280 bp in TgαSYN brains, but not in non-Tg mice brains, and the intensity of PCR products was the same level as three-, eight-, and 17-month-old Tg mice brains. (d) EGFP mRNA transcripts were detected in TgαSYN brains at the same level at three, eight and 17 months of age, but not in non-Tg mice brains (N showed non-Tg mice brains, T showed Tg mice brains). (e) The expression of human αSYN was detected as a 16 kD band at the same size as recombinant synthetic αSYN by Western blot using LB509 in LS-soluble fractions of TgαSYN #8713 (Tg1–4) mice brains, but not in three 14-month-old non-Tg mice brains (upper lane). AB5038 recognized a 16 kD band corresponding to human and mouse αSYN (lower lane). The expression level of human αSYN was about 130% of that of endogenous mouse αSYN. Synthetic αSYN (SS) was used as a marker of 16 kD αSYN (BIOMOL Research Laboratories Inc., Plymouth Meeting, PA).

was observed in the cerebellum of a 16-month-old TgαSYN (Fig. 2q). An EM study demonstrated cytoplasmic inclusions (Fig. 2r, arrow) and intranuclear inclusions (Fig. 2s, arrows) in the neurons of the brainstem. These inclusion bodies lacked the typical halo and fibrillar structure of LBs.

2.3. *Western blot analysis*

Fourteen-month-old TgαSYN showed a 16 kD band corresponding to αSYN in the LS-soluble fraction (L), Triton-soluble fraction (T), sarcosyl-soluble (S) and sarcosyl-insoluble fractions (I) (Fig. 3a: arrow). In sarcosyl-insoluble fraction, smear pattern was detected in TgαSYN#8812(T3), which accumulated much synuclein histologically. The anti-phosphorylated αSYN antibody pSyn#64 labeled the same size band as αSYN, 16 kD (Fig. 3b: arrow). These findings presented that sarcosyl-insoluble human αSYN and phosphorylated αSYN was accumulated in TgαSYN brains as reported in DLB brains (Hasegawa et al., 2002).

2.4. *Rotarod test for motor function of TgαSYN*

The rotarod test demonstrated that significant motor impairment appeared after a shorter time in TgαSYN; they dropped from the rotating rod faster than non-Tg littermates. The motor impairment was found at three months of age ($p<0.01$) and thereafter deteriorated with age ($p<0.001$. Fig. 4).

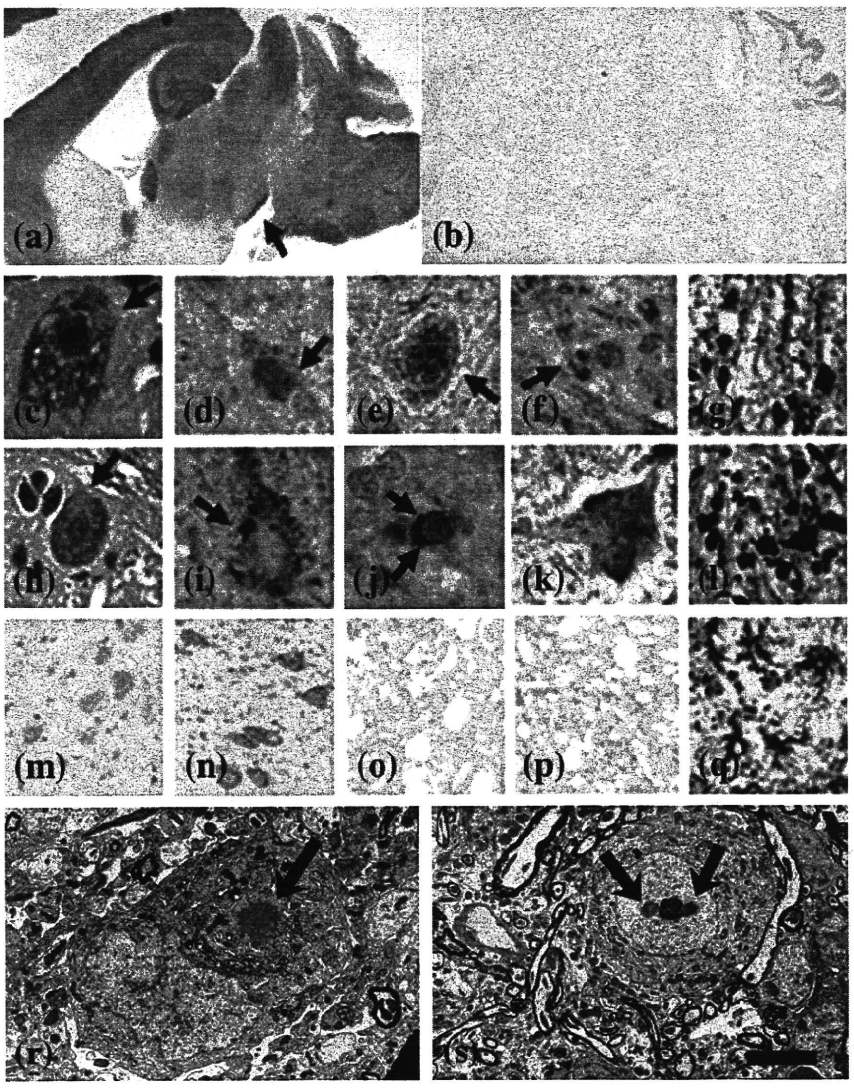

Fig. 2 – The pathological features of TgαSYN at seven months of age and age-matched non-Tg mice. (a) A sagittal section of a seven-month-old #8707 TgαSYN brain labeled by LB509 showed extensive αSYN accumulation prominently in the brainstem, hippocampus, thalamus, cerebellum and cerebral cortex. The substantia nigra of the midbrain is also labeled (arrow). The cerebral cortex and cerebellum showed atrophy. (b) No staining in the non-Tg mice brain by LB509. (c) Hematoxylin–eosin stain showed eosinophilic inclusion bodies and vacuoles in the cytoplasm of neurons in the substantia nigra of #8707 TgαSYN (arrow). (d) LB509 detected cytoplasmic inclusions in the substantia nigra of #8707 TgαSYN (arrow). (e) Anti-nitrated α/β SYN monoclonal antibody (Syn12) immunostained cytoplasmic inclusions in the substantia nigra (arrow), as well as in 14-month-old #8713 TgαSYN. (f) Ubiquitin-positive inclusions are shown in the substantia nigra of #8707 TgαSYN (arrow). (g) Ubiquitin-positive dystrophic neurites in the cerebellum dentate of 16-month-old #8713 TgαSYN. (h) Eosinophilic cytoplasmic inclusions (arrow) in the dentate nucleus of #8707 TgαSYN. (i) LB509-positive inclusion in the dentate nucleus of #8707 TgαSYN (arrow). (j) Cytoplasmic inclusions immunostained with a mouse monoclonal antibody 42/α-Synuclein in the brainstem of #8812 TgαSYN (arrow). (k) The PSer129 αSYN antibody immunostained the cytoplasm of neurons in the substantia nigra of #8707 TgαSYN. (l) Gallyas–Braak stain of dystrophic neurites in the dentate nucleus of a 16-month-old #8713 TgαSYN. (m) Tyrosine hydroxylase (TH) immuno-positive neurons in the locus ceruleus showed less immunostaining in the #8707 TgαSYN brain, than the non-Tg mouse brain (n). (o) The intensity of substance P immuno-positive synapses in the striatum of #8707 TgαSYN brain was lower than non-Tg mice brain (p). (q) Astrocytosis in the cerebellum of 16-month-old #8713 TgαSYN. (r) Electron-dense inclusions were found in the cytoplasm of neurons in the brainstems of 8-month-old #8718 TgαSYN by an EM study (arrow). (s) In the brainstem of the same mouse, intracellular inclusions (arrows) were also detected. Scale bar = 1 mm in a, b, 12.5 μm in c–f, h–k, 50 μm in g, l, m, n, 25 μm in o, p, and 0.38 μm in r, s.

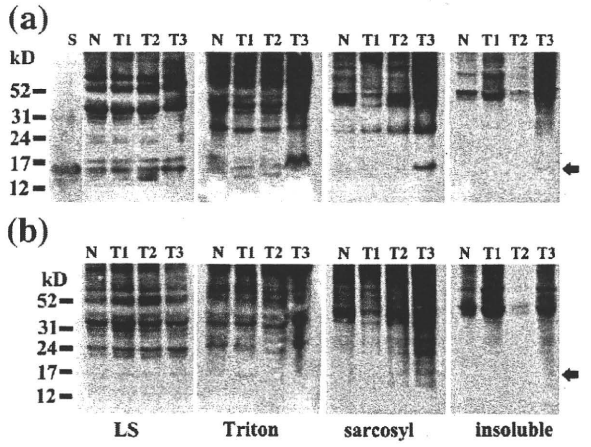

Fig. 3–Western blot analysis. The expression of human αSYN was 16 kD (lane S; corresponded to recombinant human αSYN) by Western blot using antibody LB509 (a) and pSyn#64 (b) in LS-soluble (L), Triton-soluble (T), sarcosyl-soluble (S) and sarcosyl-insoluble (I) fractions of non-Tg (N), TgαSYN#8713 (T1), TgαSYN#8819 (T2), and TgαSYN#8812 (T3), 14-month-old mice brains.

2.5. *Measurement of neurochemicals*

There was no significant difference in brain weight among Tg and non-Tg mice at 10 and 17 months of age. Compared with age-matched non-Tg control mice, the levels of DA in the striatum were significantly decreased in 10 month-old ($p=0.0159$) and 17 month-old mice brains ($p=0.0286$). DA decreased approximately 17% to 24% in the striatum of TgαSYN brains (Fig. 5a). A significant decrease in DA was also detected in the hypothalamuses of 17-month-old TgαSYN brains ($p=0.0079$. Fig. 5b). NE was not decreased in any areas of 10-month-old TgαSYN brains (Fig. 5c). Serotonin was decreased in the hypothalamuses of 10- and 17-month-old TgαSYN brains ($p=0.0079$, $p=0.0286$, respectively. Fig. 5d). ACh decreased in the striatum in 17-month-old TgαSYN ($p=0.0286$. Fig. 5e). There was no significant alteration in DOPAC, HVA, MHPG, 5-HIAA and Ch levels in any areas of TgαSYN (data not shown). These results showed that insoluble mutant αSYN aggregation selectively decreased the DA level at 10 and 17 months of age.

3. Discussion

Several groups have already reported animal models of PD, such as wild-type αSYN Tg mice (Masliah et al., 2000), mutant αSYN Tg mice (van der Putten et al., 2000, Kahle et al., 2000, Giasson et al., 2002, Lee et al., 2002, Richfield et al., 2002, Neumann et al., 2002, Thiruchelvam et al., 2004, Tofaris et al. 2006, Wakamatsu et al., 2008), *Drosophila melanogaster* (Pendleton et al., 2002) and *C. elegans* (Kuwahara et al., 2006). The first αSYN Tg mice expressed wild-type human αSYN driven by the PDGF-β promoter (Masliah et al., 2000). This mouse displayed intraneuronal inclusions immunoreactive for αSYN and ubiquitin in several regions typically affected in α-synucleinopathies, while lacking the characteristic fibrillar components of Lewy bodies. The Tg mice overexpressing αSYN A53T developed under the murine Thy-1 regulatory sequence showed an early and dramatic decline in motor function (van der Putten et al., 2000). Transgenic wild-type and A30P αSYN abnormally accumulated in neuronal cell bodies and neurites throughout the brain (Kahle et al., 2000). Mice expressing wild-type or A53T αSYN under the mouse prion promoter developed motor deficits by eight months of age (Giasson et al., 2002). Neuropathological assessment of these Tg mice revealed a wide distribution of αSYN, with a pathological sparing of the motor cortex and a total sparing of the substantia nigra. Another group developed Tg mice harboring αSYN A53T using a mouse prion promoter showing motor dysfunction and αSYN accumulation (Lee et al., 2002). Truncated human αSYN (C-120) Tg mice under the TH promoter led to pathological changes in dopaminergic nerve cells of the substantia nigra and olfactory bulb (Tofaris et al., 2006). Recently, truncated human αSYN (C-130) Tg mice also led to selective loss of dopaminergic neurons and accumulation of phosphorylated αSYN (Wakamatsu et al., 2007, 2008).

One of the differences between these models and our TgαSYN was a novel combination of a promoter and mutation of αSYN. TgαSYN expressed double mutant αSYN with A30P +A53T under the human Thy-1 promoter. As expected, our TgαSYN demonstrated widespread αSYN accumulation in the brainstem, caudate putamen, cerebellum, hippocampus and cerebral cortex. Eosinophilic inclusion bodies in the substantia nigra and dentate nucleus of the cerebellum corresponded to accumulation of αSYN. Accumulated αSYN was ubiquitinated, nitrated and phosphorylated at the histological levels as shown in PD and DLB brain. Unfortunately, these inclusion bodies were not compatible with typical LBs because of the absence of a halo structure. At the EM level, fibrillar structure was not observed in inclusion bodies, but they were composed of massive aberrant fine granular structures. Aberrant inclusion bodies with modified αSYN were also observed widely. Since Gallyas–Braak staining labeled these LNs, accumulated αSYN in these neurites may have characteristics of those in β-sheet pleated structures.

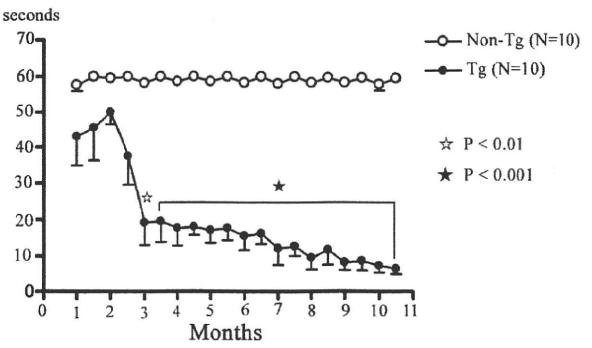

Fig. 4–Rotarod test. The retention time of Tg mice on the rotarod significantly decreased in TgαSYN. The significant difference began to decrease at three months old (☆: $p<0.01$) and progressively deteriorated in an age-dependent manner from six months (★: $p<0.001$). Statistics were analyzed by two-way repeated measures ANOVA.

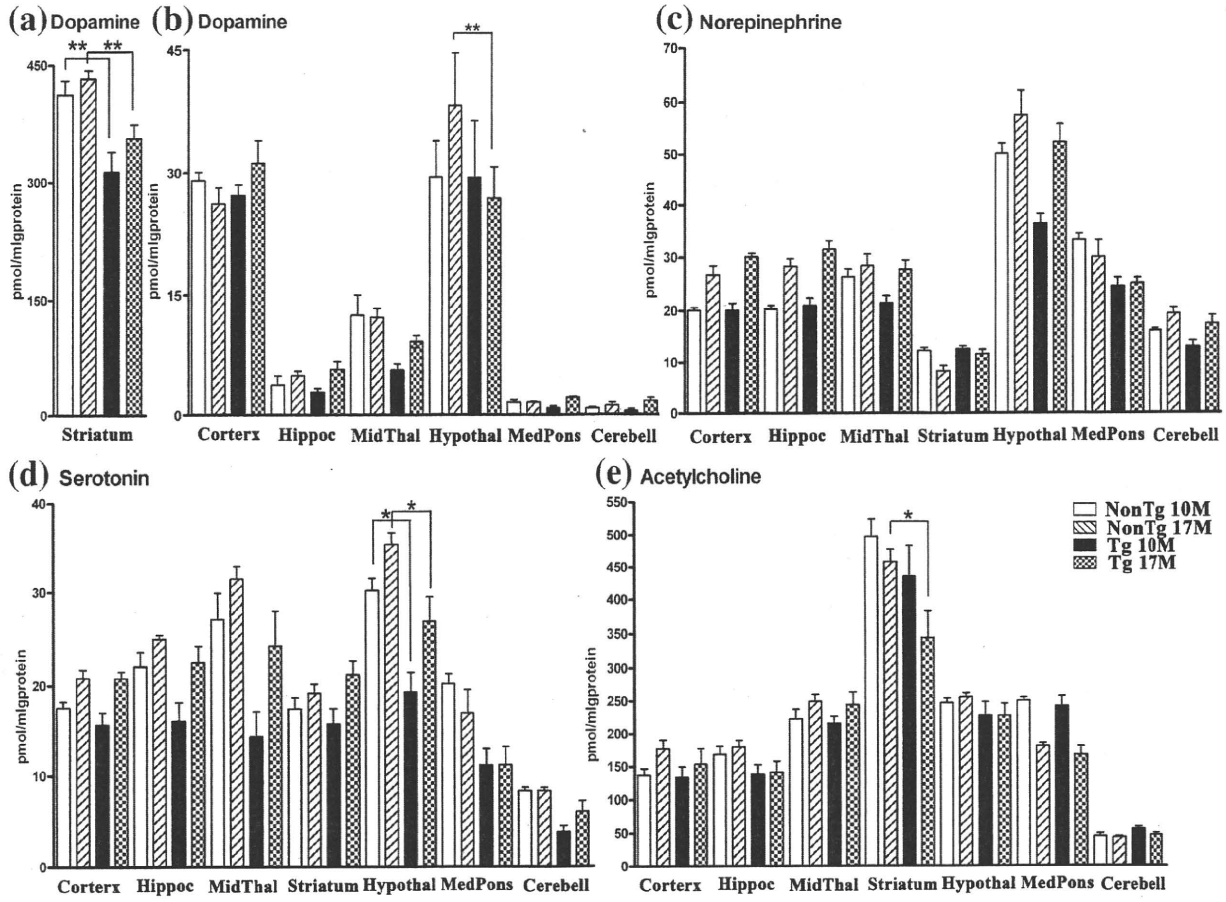

Fig. 5 – Measurement of neurochemicals. Opened column: 10-month-old non-Tg mice, Oblique column: 17-month-old non-Tg mice; Closed black colored column: 10-month-old TgαSYN mice, Crossed column: 17-month-old non-Tg mice. Cortex: cerebral cortex, Hippoc: hippocampus, MidThal: midbrain–thalamus, Hypothal: hypothalamus, MedPons: medulla–pons, Cerebell: cerebellum. *$p<0.01$, **$p<0.05$. Statistical analysis of neurochemicals between the TgαSYN and non-Tg control groups at the same age was conducted by a two-way repeated measure ANOVA (GraphPad Prism 4). (a) DA was significantly decreased in the striatum in 10- and 17-month-old TgαSYN compared with non-Tg control mice. (b) A decrease in dopamine was detected significantly in the hypothalamuses of 17-month-old TgαSYN brains ($p=0.0079$). (c) Norepinephrine (NE) was not decreased in 10- and 17-month-old TgαSYN brains. (d) Serotonin (5-HT) was decreased in the hypothalamus of 10- and 17-month-old TgαSYN brains ($p=0.0079$, $p=0.0286$, respectively). (e) ACh was decreased in the striatum of 17-month-old TgαSYN ($p=0.0286$).

The α-synuclein pathologies in TgαSYN were accompanied by decreased tyrosine hydroxylase-positive neurons, Substance P synapses and severe astrocytosis. These histological α-synuclein pathologies were also detected at the biochemical level. Accumulated αSYN was phosphorylated, ubiquitinated and sarcosyl-insoluble, suggesting that it may be conformationally changed as reported in PD/DLB brains (Hasegawa et al., 2002). The presence of higher molecule phosphorylated and ubiquitinated bands (22/29 kD) on Western blots also indicated that accumulated αSYN was modified and aggregated.

The severe decrease in DA and loss of dopaminergic neurons in SNc and the striata of PD brains is widely believed to be the pathological and biochemical cause of PD. Notably, our TgαSYN demonstrated decreased DA production in a disturbed DA system which was measured in the liquid chromatographic systems. Although other neurochemicals were altered slightly, a prominently decreased level of DA was revealed in the striatum of TgαSYN. These findings suggest selective neurotoxicity with αSYN accumulation.

In our mouse model, approximately a 20% reduction in DA in the striatum was observed when motor impairment existed. Since the rotarod test revealed significant decreased spontaneous movement, the phenotype of TgαSYN is quite similar to the cardinal clinical symptom of PD, akinesia. A decreased level of TH-positive neurons and substance P synapses also suggested that the motor impairment in TgαSYN may be caused by aberrant αSYN processes.

Our TgαSYN is a mammalian model animal showing decreased DA and motor deficits, which were certainly detected by the liquid chromatographic systems and rotarod test. For this reason, TgαSYN is a useful model for analyzing the aberrant cascade induced by pathological metabolism and aggregation of mutant αSYN, and may be useful for developing essential treatments for α-synucleinopathies such as PD and DLB.

4. Experimental procedures

4.1. *Transgene construction, generation of transgenic mice and analyses of RT-PCR*

Human αSYN A30P+A53T cDNA (450 bp) was ligated into Hind III sites in the human Thy-1 genome gene. The transgene hThy1-αSYN A30P+A53T consisted of an 8.1 kb XhoI–NcoI fragment of pBluescript II KS kidney enhancer (Fig. 1a). The CX-EGFP transgene consisted of a 3 kb Xba I/BamH I fragment of pCAGGS containing the CMV enhancer, β-actin promoter, a part of the rabbit β-globin gene, a part of the second intron, the third exon and 3′-untranslated region and cDNA of EGFP (Enhanced green fluorescent protein) with the Kozak sequence (Imai et al., 1999). Approximately 2,000 copies of the transgene with a 1:1 mole rate mixture of the hThy1-αSYN A30P+A53T and CX-EGFP as a transgene marker were micro-injected into the pronuclei of fertilized BDF1 eggs. To analyze gene expression of human αSYN, RT-PCR was performed using 2 μl of mRNA, isolated using the QuickPrep Micro mRNA purification kit (GE Healthcare Bio-Sciences Corp., Piscataway, NJ), from the brains of TgαSYN (#8713) and non-Tg mice brains at 3, 8, 17 months of age ($n=3$, respectively) in the reaction tube of Ready-To-Go RT-PCR Beads (GE Healthcare Bio-Sciences Corp., Piscataway, NJ) with PCR primer sets as follows: (αSYN forward primer: TG GAT GTA TTC ATG AAA GGA, αSYN reverse primer: CC AGT GGC TGC TGC AAT GCT C; EGFP forward primer: TGG TGA GCA AGG GCG AGG AG; EGFP reverse primer: TCG TGC TGC TTC ATG TGG TC). For semi-quantification, RT-PCR of β-actin was performed as an internal control (Elliott, 2001). Ten microliters of PCR products were analyzed by 2.5% agarose gel electrophoresis. The intensity of ethidium-stained bands was analyzed by Scion Image (Scion Corporation, Frederick, MD).

4.2. *Histological examinations*

After mice were sacrificed under anesthesia, the brains were removed and cut sagittally along the midline. One hemisphere was fixed in 0.1 mol/L phosphate buffer (PB, pH 7.6) containing 4% paraformaldehyde, and embedded in paraffin. For immunostaining, 5-μm sections were treated with 99% formic acid for 3 min, or treated in a microwave at 500 W for 5 min three times in 10 mmol/L citrate buffer (pH 6.0). After blocking with 5% normal goat or horse serum in 50 mmol/L phosphate buffered saline (PBS) containing 0.05% Tween-20 and 4% Block-Ace (Snow brand, Sapporo, Japan), sections were incubated with primary antibodies for 6 h. Specific labeling was visualized using a Vectastain Elite ABC kit (Vector, Burlingame, CA). Immunostained tissue sections were counterstained with hematoxylin. Nissl, Hematoxylin–eosin (H–E), and Gallyas–Braak stains were also done.

The following antibodies were used: mouse monoclonal antibody to human αSYN, LB509 (×4, residues 115–121/122) (Baba et al., 1998); mouse monoclonal antibody to αSYN, 42/α-Synuclein (×50, BD Transduction Laboratories, San Jose, CA); rabbit polyclonal antibody to phosphorylated Serine at residue 129 of human αSYN, PSer129 (×200) (Fujiwara et al., 2002; Hasegawa et al., 2002); rabbit polyclonal antibody to tyrosine hydroxylase (TH), AB151 (×2,000, CHEMICON, Temecula, CA); rabbit polyclonal antibody to substance P, AB1566 (×1,000, CHEMICON, Temecula, CA); rabbit polyclonal antibody to ubiquitin, UbiQ (×500) (Ikeda et al., 2005; Murakami et al., 2006); mouse monoclonal antibody to nitrated α/β SYN, Syn12 (×400, Invitrogen, Corps., Carlsbad, CA); rabbit polyclonal antibody to glial fibrillary acidic protein (GFAP, ×20,000, DAKO, Carpinteria, CA).

For electron microscopic (EM) studies, the brain tissues were immersed in a fixative solution (2.5% glutaraldehyde, 0.1 mol/L phosphate buffer (PB), pH 7.4) for 4 h and washed several times in 0.1 mol/L PB containing 7% sucrose. Blocks were then postfixed in 2% osmium tetroxide, dehydrated in ethanol and propylene oxide, and embedded in Quetol 812 (Nisshin EM, Tokyo, Japan). Ultrathin sections were stained with uranyl acetate and lead acetate prior to observation.

4.3. *Western blot analysis*

Half of each brain was homogenized in 3 ml/g of low-salt buffer (LS: 10 mmol/L Tris, 5 mmol/L ethylenediaminetetraacetic acid (EDTA), 1 mmol/L dithiothreitol (DTT), 10% sucrose, and a cocktail of protease inhibitors (Complete®, Roche Diagnostics, Indianapolis, IN), pH 7.5) and centrifuged at 25,000 g for 30 min at 4 °C (LS-soluble fraction). Pellets were treated with 3 ml/g of LS with 1% Triton X-100 and 0.5 mol/L NaCl, and centrifuged at 180,000 g for 30 min at 4 °C (Triton-soluble fraction). Pellets were then homogenized again in 2 ml/g LS with 1% N-lauroylsarcosine (SIGMA CHEMICAL CO. St Louis, MO) and 0.5 mol/L NaCl, incubated at 22 °C on a shaker for 1 h, and centrifuged at 180,000 g for 30 min at 22 °C. Supernatants were analyzed as sarcosyl-soluble fraction (Iwatsubo et al., 1996; Hasegawa et al., 2002; Sampathu et al., 2003; Ikeda et al., 2005; Murakami et al., 2006). The remaining pellets obtained from each sarcosyl-insoluble fraction were boiled at 70 °C in 20 μl of NuPAGE® LDS Sample Buffer for 10 min. Each fraction was separated on 4 to 12% NuPAGE Bis–Tris Gels (Invitrogen, Corps., Carlsbad, CA) and the blots were labeled by a mouse monoclonal antibody to human αSYN (LB509, ×4), and a mouse monoclonal antibody to phosphorylated Serine at residue 129 of human αSYN (pSyn#64, ×200, Wako, Japan). Signals were visualized with an enhanced chemiluminescence detection system (SuperSignal West® Dura Extended Duration Substrate, PIERCE, Rockford, IL) and quantified by a luminoimage analyzer (LAS 1000-mini, Fuji film, Tokyo, Japan).

4.4. *Measurement of neurochemicals*

Neurochemicals, including dopaminergic (dopamine: DA, 3,4-dihydroxyphenylacetic acid: DOPAC, homovanillic acid: HVA), noradrenergic (norepinephrine: NE, 3-methoxy-4hydroxyphenylglycol: MHPG), serotonergic (5-hydroxytryptamine: 5-HT, 5-hydroxyindoleacetic acid: 5-HIAA) and cholinergic (acetylcholine: ACh, choline: Ch) systems in the brain were measured in Tg mice ($n=10$) and non-Tg control mice ($n=10$) at 10 and 17 months old, respectively. In brief, each animal was anesthetized with Nembutal® (Dainippon Pharmaceutical Co. Ltd., pentobarbital sodium), sacrificed, and irradiated with microwaves (NJE 2603 Microwave device, New Japan Radio, Kamifukuoka, Japan) at 9.0 kW for 0.42 s to prevent post-mortem

changes in the neurochemicals during brain sampling (Ikarashi et al., 1985, 2004). The brain was removed from the skull and dissected into seven regions (cerebral cortex, hippocampus, midbrain–thalamus, striatum, hypothalamus, medulla–pons and cerebellum) according to the established method (Glowinski and Iversen, 1966), and then each region was weighed. Each dissected brain region was homogenized with 0.5 ml of 0.1 mol/L perchloric acid containing 0.8 nmol isoproterenol hydrochloride as an internal standard for the determinations of catecholamines, indoleamines and related metabolites, and 5 nmol ethylhomocholine iodide as an internal standard for the determinations of ACh and Ch, using an ultrasonic cell disrupter (US-300T, Nissei, Tokyo, Japan). The homogenate was centrifuged at 17,300 g at 4 °C for 15 min. The supernatant was filtered through a 0.45 μm millipore filter. Aliquots, typically 10 μl of the filtrates, were injected into the liquid chromatographic systems (Eicom HPLC-ECD system, Eicom Co. Ltd., Kyoto, Japan) to determine catecholamines-, indoleamines-, and acetylcholine-related substances (Ikarashi et al., 1992). The sediment was re-homogenized with 2 ml of 1 mol/L NaOH for a protein assay, which was performed using the method of Lowry et al. (1951). The concentrations of neurochemicals in the brain were expressed as the values per milligram of protein.

4.5. *Behavioral experiments*

4.5.1. *Rotarod test*

TgαSYN (n=10) and age-matched control mice (n=10) at one month to 10.5 months old were examined by the rotarod performance test according to a previous method (Kuribara et al., 1977; Ikarashi et al., 2004). Mice were placed on the rotating rod of the apparatus (Ugo basile, biological research apparatus, Milan, Italy) at a speed of 16 rpm for 300 s, and the time they stayed on the rotating rod was measured. Each set of three trials was performed at 10 minute intervals each day for every mouse.

4.6. *Statistical analyses*

Two-way repeated measures ANOVA followed by the Mann–Whitney U test for the rotarod test and open field test, and two-way ANOVA followed by Student's t test to analyze neurochemicals were performed using GraphPad Prism 4 (GraphPad Software Inc., San Diego, CA) and SPSS 10.0 (SPSS 10.0 for Windows, SPSS Inc., Chicago, IL). The means of all data are presented with their standard errors (mean±S.E.).

Acknowledgments

We thank Dr. T Iwatsubo for coordinative provision of the LB 509 antibody and polyclonal phosphorylated αSYN antibody, Dr. D Dickson for the antibody Ubi-Q and Dr. S Kawabata for the human Thy-1 gene. We thank Dr. H Sugimoto and Dr. T Izumi for technical supports, and Dr. J Hirato for kind coordinative support. We also thank Y Nogami and H Narihiro for technical assistance. All animal experiments were performed according to guidelines established in the "Guide for the Care and Use of Laboratory Animals" (Japan).

REFERENCES

Abeliovich, A., Schmitz, Y., Farinas, I., Choi-Lundberg, D., Ho, W.H., Castillo, P.E., Shinsky, N., Verdugo, J.M., Armanini, M., Ryan, A., Hynes, M., Phillips, H., Sulzer, D., Rosenthal, A., 2000. Mice lacking α-synuclein display functional deficits in the nigrostriataL-DOPAmine system. Neuron 25, 239–252.

Arai, K., Kato, N., Kashiwado, K., Hattori, T., 2000. Pure autonomic failure in association with human α-synucleinopathy. Neurosci. Lett. 296, 171–173.

Baba, M., Nakajo, S., Tu, P.H., Tomita, T., Nakaya, K., Lee, V.M., Trojanowski, J.Q., Iwatsubo, T., 1998. Aggregation of α-synuclein in Lewy bodies of sporadic Parkinson's disease and dementia with Lewy bodies. Am. J. Pathol. 152, 879–884.

Chartier-Harlin, M.C., Kachergus, J., Roumier, C., Mouroux, V., Douay, X., Lincoln, S., Levecque, C., Larvor, L., Andrieux, J., Hulihan, M., Waucquier, N., Defebvre, L., Amouyel, P., Farrer, M., Destée, A., 2004. -Synuclein locus duplication as a cause of familial Parkinson's disease. Lancet 364, 1167–1169.

Chen, X., de Silva, H.A., Pettenati, M.J., Rao, P.N., St. George-Hyslop, P., Roses, A.D., Xia, Y., Horsburgh, K., Ueda, K., Saitoh, T., 1995. The human NACP/α-synuclein gene: chromosome assignment to 4q21.3–q22 and TaqI RFLP analysis. Genomics 26, 425–427.

Chishti, M.A., Yang, D.S., Janus, C., Phinney, A.L., Horne, P., Pearson, J., Strome, R., Zuker, N., Loukides, J., French, J., Turner, S., Lozza, G., Grilli, M., Kunicki, S., Morissette, C., Paquette, J., Gervais, F., Bergeron, C., Fraser, P.E., Carlson, G.A., George-Hyslop, P.S., Westaway, D., 2001. Early-onset amyloid deposition and cognitive deficits in transgenic mice expressing a double mutant form of amyloid precursor protein 695. J. Biol. Chem. 276, 21562–21570.

Choi, W., Zibaee, S., Goedert, M., 2004. Mutation increases phospholipids binding and assembly into filaments of human α-synuclein. FEBS Lett. 576, 363–368.

Citron, M., Eckman, C.B., Diehl, T.S., Corcoran, C., Ostaszewski, B. L., Xia, W., Levesque, G., St. George-Hyslop, P., Younkin, S.G., Selkoe, D.J., 1998. Additive effects of PS1 and APP mutations on secretion of the 42-residue amyloid β-protein. Neurobiol. Dis. 5, 107–116.

Clayton, D.F., George, J.M., 1998. The synucleins: a family of proteins involved in synaptic function, plasticity, neurodegeneration and disease. Trends. Neurosci. 21, 249–254.

Conway, K.A., Rochet, J.C., Bieganski, R.M., Lansbury Jr., P.T., 2001. Kinetic stabilization of the α-synuclein protofibril by a dopamine-α-synuclein adduct. Science 294, 1346–1349.

Elliott, J.L., 2001. Cytokine upregulation in a murine model of familial amyotrophic lateral sclerosis. Brain Res. Mol. Brain Res. 95, 172–178.

Fujiwara, H., Hasegawa, M., Dohmae, N., Kawashima, A., Masliah, E., Goldberg, M.S., Shen, J., Takio, K., Iwatsubo, T., 2002. -Synuclein is phosphorylated in synucleinopathy lesions. Nat. Cell Biol. 4, 160–164.

Galvin, J.E., Giasson, B., Hurtig, H.I., Lee, V.M., Trojanowski, J.Q., 2000. Neurodegeneration with brain iron accumulation, type 1 is characterized by α-, β-, and γ-synuclein neuropathology. Am. J. Pathol. 157, 361–368.

George, J.M., Jin, H., Woods, W.S., Clayton, D.F., 1995. Characterization of a novel protein regulated during the critical period for song learning in the zebra finch. Neuron 15, 361–372.

Giasson, B.I., Duda, J.E., Quinn, S.M., Zhang, B., Trojanowski, J.Q., Lee, V.M., 2002. Neuronal α-Synucleinopathy with severe movement disorder in mice expressing A53T human α-synuclein. Neuron 34, 521–533.

Glowinski, J., Iversen, L.L., 1966. Regional studies of catecholamines in the rat brain. I. The disposition of [^{3}H]norepinephrine, [^{3}H]dopamine and [^{3}H]dopa in various regions of the brain. J. Neurochem. 13, 655–669.

Goedert, M., 2000. -synuclein and neurodegenerative diseases. Nat. Rev. Neurosci. 2, 492–501.
Hardy, J., Gwinn-Hardy, K., 1998. Genetic classification of primary neurodegenerative disease. Science 282, 1075–1079.
Hasegawa, M., Fujiwara, H., Nonaka, T., Wakabayashi, K., Takahashi, H., Lee, V.M., Trojanowski, J.Q., Mann, D., Iwatsubo, T., 2002. Phosphorylated α-synuclein is ubiquitinated in alpha-synucleinopathy lesions. J. Biol. Chem. 277, 49071–49076.
Ikarashi, Y., Harigaya, Y., Tomidokoro, Y., Kanai, M., Ikeda, M., Matsubara, E., Kawarabayashi, T., Kuribara, H., Younkin, S.G., Maruyama, Y., Shoji, M., 2004. Decreased level of brain acetylcholine and memory disturbance in APPsw mice. Neurobiol. Aging 25, 483–490.
Ikarashi, Y., Sasahara, T., Maruyama, Y., 1985. Postmortem changes in catecholamines, indoleamines, and their metabolites in rat brain regions: prevention with 10-kW microwave irradiation. J. Neurochem. 45, 935–939.
Ikarashi, Y., Blank, C.L., Maruyama, Y., 1992. Glassy carbon pre-column for determination of acetylcholine and choline in biological samples using liquid chromatography with electrochemical detection. J. Chromatogr. 575, 29–37.
Ikeda, M., Shoji, M., Kawarai, T., Kawarabayashi, T., Matsubara, E., Murakami, T., Sasaki, A., Tomidokoro, Y., Ikarashi, Y., Kuribara, H., Ishiguro, K., Hasegawa, M., Yen, S.H., Chishti, M.A., Harigaya, Y., Abe, K., Okamoto, K., St George-Hyslop, P., Westaway, D., 2005. Accumulation of filamentous tau in the cerebral cortex of human tau R406W transgenic mice. Am. J. Pathol. 166, 521–531.
Imai, E., Akagi, Y., Isaka, Y., Ikawa, M., Takenaka, M., Hori, M., Okabe, M., 1999. Glowing podocytes in living mouse: transgenic mouse carrying a podocyte-specific promoter. Exp. Nephrol. 7, 63–66.
Iwai, A., Masliah, E., Yoshimoto, M., Ge, N., Flanagan, L., de Silva, H. A., Kittel, A., Saitoh, T., 1995. The precursor protein of non-Aβ component of Alzheimer's disease amyloid is a presynaptic protein of the central nervous system. Neuron 14, 467–475.
Iwatsubo, T., Yamaguchi, H., Fujimuro, M., Yokosawa, H., Ihara, Y., Trojanowski, J.Q., Lee, V.M., 1996. Purification and characterization of Lewy bodies from the brains of patients with diffuse Lewy body disease. Am. J. Pathol. 148, 1517–1529.
Kahle, P.J., Neumann, M., Ozmen, L., Muller, V., Jacobsen, H., Schindzielorz, A., Okochi, M., Leimer, U., van der Putten, H., Probst, A., Kremmer, E., Kretzschmar, H.A., Haass, C., 2000. Subcellular localization of wild-type and Parkinson's disease-associated mutant α-synuclein in human and transgenic mouse brain. J. Neurosci. 20, 6365–6373.
Kitada, T., Asakawa, S., Hattori, N., Matsumine, H., Yamamura, Y., Minoshima, S., Yokochi, M., Mizuno, Y., Shimizu, N., 1998. Mutations in the parkin gene cause autosomal recessive juvenile parkinsonism. Nature 392, 605–608.
Kruger, R., Kuhn, W., Muller, T., Woitalla, D., Graeber, M., Kosel, S., Przuntek, H., Epplen, J.T., Schols, L., Riess, O., 1998. Ala30Pro mutation in the gene encoding α-synuclein in Parkinson's disease. Nat. Genet. 18, 106–108.
Kuribara, H., Higuchi, Y., Tadokoro, S., 1977. Effects of central depressants on rota-rod and traction performances in mice. Jpn. J. Pharmacol. 27, 117–126.
Lee, M.K., Stirling, W., Xu, Y., Xu, X., Qui, D., Mandir, A.S., Dawson, T.M., Copeland, N.G., Jenkins, N.A., Price, D.L., 2002. Human α-synuclein-harboring familial Parkinson's disease-linked Ala-53. Thr mutation causes neurodegenerative disease with α-synuclein aggregation in transgenic mice. Proc. Natl. Acad. Sci. U. S. A. 99, 8968–8973.
Liscovitch, M., Czarny, M., Fiucci, G., Tang, X., 2000. Phospholipase D: molecular and cell biology of a novel gene family. Biochem. J. 345, 401–415.
Lotharius, J., Brundin, P., 2000. Pathogenesis of Parkinson's disease: dopamine, vesicles and α-synuclein. Nat. Rev. Neurosci. 3, 932–942.
Lowry, O.H., Rosebrough, N.J., Farr, A.L., Randall, R.J., 1951. Protein measurement with the Folin phenol reagent. J. Biol. Chem. 193, 265–275.
Masliah, E., Rockenstein, E., Veinbergs, I., Mallory, M., Hashimoto, M., Takeda, A., Sagara, Y., Sisk, A., Mucke, L., 2000. L-DOPAminergic loss and inclusion body formation in α-synuclein mice: implications for neurodegenerative disorders. Science 287, 1265–1269.
Murakami, T., Paitel, E., Kawarabayashi, T., Ikedame>M., Chishti, M.A., Janus, C., Matsubara, E., Sasaki, A., Kawarai, T., Phinney, A.L., Harigaya, Y., Horne, P., Egashira, N., Mishima, K., Hanna, A., Yang, J., Iwasaki, K., Takahashi, M., Fujiwara, M., Ishiguro, K., Bergeron, C., Carlson, G.A., Abe, K., Westaway, D., St. George-Hyslop, P., Shoji, M., 2006. Cortical neuronal and glial pathology in TgTauP301L transgenic mice: neuronal degeneration, memory disturbance, and phenotypic variation. Am. J. Pathol. 169, 1343–1352.
Neumann, M., Kahle, P.J., Giasson, B.I., Ozmen, L., Borroni, E., Spooren, W., Muller, V., Odoy, S., Fujiwara, H., Hasegawa, M., 2002. Misfolded proteinase K-resistant hyperphosphorylated α-synuclein in aged transgenic mice with locomotor deterioration and in human α-synucleinopathies. J. Clin. Invest. 110, 1429–1439.
Payton, J.E., Perrin, R.J., Woods, W.S., George, J.M., 2000. Structural determinants of PLD2 inhibition by α-synuclein. J. Mol. Biol. 337, 1001–1009.
Polymeropoulos, M.H., Lavedan, C., Leroy, E., Ide, S.E., Dehejia, A., Dutra, A., Pike, B., Root, H., Rubenstein, J., Boyer, R., Stenroos, E.S., Chandrasekharappa, S., Athanassiadou, A., Papapetropoulos, T., Johnson, W.G., Lazzarini, A.M., Duvoisin, R.C., Di Iorio, G., Golbe, L.I., Nussbaum, R.L., 1997. Mutation in the α-synuclein gene identified in families with Parkinson's disease. Science 276, 2045–2047.
Richfield, E.K., Thiruchelvam, M.J., Cory-Slechta, D.A., Wuertzer, C., Gainetdinov, R.R., Caron, M.G., Di Monte, D.A., Federoff, H.J., 2002. Behavioral and neurochemical effects of wild-type and mutated human alpha-synuclein in transgenic mice. Exp. Neurol. 175, 35–48.
Sampathu, D.M., Giasson, B.I., Pawlyk, A.C., Trojanowski, J.Q., Lee, V.M., 2003. Ubiquitination of α-synuclein is not required for formation of pathological inclusions in α-synucleinopathies. Am. J. Pathol. 163, 91–100.
Shimura, H., Schlossmacher, M.G., Hattori, N., Frosch, M.P., Trockenbacher, A., Schneider, R., Mizuno, Y., Kosik, K.S., Selkoe, D.J., 2001. Ubiquitination of a new form of α-synuclein by parkin from human brain: implications for Parkinson's disease. Science 293, 263–269.
Shoji, M., Harigaya, Y., Sasaki, A., Ueda, K., Ishiguro, K., Matsubara, E., Watanabe, M., Ikeda, M., Kanai, M., Tomidokoro, Y., Shizuka, M., Amari, M., Kosaka, K., Nakazato, Y., Okamoto, K., Hirai, S., 2000. Accumulation of NACP/α-synuclein in Lewy body disease and multiple system atrophy. J. Neurol. Neurosurg. Psychiatry 68, 605–608.
Singleton, A.B., Farrer, M., Johnson, J., Singleton, A., Hague, S., Kachergus, J., Hulihan, M., Peuralinna, T., Dutra, A., Nussbaum, R., Lincoln, S., Crawley, A., Hanson, M., Maraganore, D., Adler, C., Cookson, M.R., Muenter, M., Baptista, M., Miller, D., Blancato, J., Hardy, J., Gwinn-Hardy, K., 2002. -Synuclein locus triplication causes Parkinson's disease. Science 302, 841.
Spillantini, M.G., Schmidt, M.L., Lee, V.M., Trojanowski, J.Q., Jakes, R., Goedert, M., 1997. -synuclein in Lewy bodies. Nature 388, 839–840.
Thiruchelvam, M.J., Powers, J.M., Cory-Slechta, D.A., Richfield, E.K., 2004. Risk factors for dopaminergic neuron loss in human α-synuclein transgenic mice. Eur. J. Neurosci. 19, 845–854.
Tofaris, G.K., Reitböck, P.G., Humby, T., Lambourne, S.L., O'Connell, M., Ghetti, B., Gossage, H., Emson, P.C., Wilkinson, L.S., Goedert, M., Spillantini, M.G., 2006. Pathological changes in dopaminergic nerve cells of the substantia nigra and olfactory bulb in mice transgenic for truncated human

α-synuclein(1–120): implications for Lewy body disorders. J. Neurosci. 26, 3942–3950.

Tu, P.H., Galvin, J.E., Baba, M., Giasson, B., Tomita, T., Leight, S., Nakajo, S., Iwatsubo, T., Trojanowski, J.Q., Lee, V.M., 1998. Glial cytoplasmic inclusions in white matter oligodendrocytes of multiple system atrophy brains contain insoluble α-synuclein. Ann. Neurol. 44, 415–422.

Ueda, K., Fukushima, H., Masliah, E., Xia, Y., Iwai, A., Yoshimoto, M., Otero, D.A., Kondo, J., Ihara, Y., Saitoh, T., 1992. Molecular cloning of cDNA encoding an unrecognized component of amyloid in Alzheimer disease. Proc. Natl. Acad. Sci. U. S. A. 90, 11282–11286.

van der Putten, H., Wiederhold, K.H., Probst, A., Barbieri, S., Mistl, C., Danner, S., Kauffmann, S., Hofele, K., Spooren, W.P., Ruegg, M.A., Lin, S., Caroni, P., Sommer, B., Tolnay, M., Bilbe, G., 2000. Neuropathology in mice expressing human α-synuclein. J. Neurosci. 20, 6021–6029.

Wakamatsu, M., Ishii, A., Ukai, Y., Sakagami, J., Iwata, S., Ono, M., Matsumoto, K., Nakamura, A., Tada, N., Kobayashi, K., Iwatsubo, T., Yoshimoto, M., 2007. Accumulation of phosphorylated α-synuclein in dopaminergic neurons of transgenic mice that express human α-synuclein J. Neurosci. Res. 85, 1819–1825.

Wakamatsu, M., Ishii, A., Iwata, S., Sakagami, J., Ukai, Y., Ono, M., Kanbe, D., Muramatsu, S., Kobayashi, K., Iwatsubo, T., Yoshimoto, M., 2008. Selective loss of nigral dopamine neurons induced by overexpression of truncated human α-synuclein in mice. Neurobiol. Aging 29, 574–585.

Zarranz, J.J., Alegre, J., Gomez-Esteban, J.C., Lezcano, E., Ros, R., Ampuero, I., Vidal, L., Hoenicka, J., Rodriguez, O., Atares, B., Llorens, V., Gomez Tortosa, E., del Ser, T., Munoz, D.G., de Yebenes, J.G., 2004. The new mutation, E46K, of α-synuclein causes Parkinson and Lewy body dementia. Ann. Neurol. 55, 164–173.

Journal of Neuroimmunology 214 (2009) 93–100

Contents lists available at ScienceDirect

Journal of Neuroimmunology

journal homepage: www.elsevier.com/locate/jneuroim

Fingolimod and related compounds in a spontaneous autoimmune polyneuropathy

Hye-Jung Kim [a], Cha-Gyun Jung [a], Danuta Dukala [a], Hyun Bae [a], Rafael Kakazu [a], Robert Wollmann [b], Betty Soliven [a,*]

[a] Department of Neurology, The University of Chicago, Chicago, IL, United States
[b] Dept. of Pathology, The University of Chicago, Chicago, IL, 5841 S. Maryland Ave, Chicago, IL 60637, United States

ARTICLE INFO

Article history:
Received 6 June 2009
Received in revised form 3 July 2009
Accepted 6 July 2009

Keywords:
CIDP
Guillain–Barré syndrome
S1P receptors
NOD mice
FTY720
SEW2871

ABSTRACT

We investigated potential therapeutic effects of sphingosine-1-phosphate (S1P) receptor modulators FTY720 (fingolimod) and selective S1P1 agonist SEW2871 on a spontaneous autoimmune polyneuropathy (SAP) when given orally at 7 mo (anticipated disease onset) for 4 weeks. Clinical severity, electrophysiologic and histological findings were ameliorated in mice treated with 1 mg/kg of FTY720. Subsequent studies showed that SEW2871 was also effective in halting the progression of SAP, which was accompanied by decreased proliferative and cytokine responses to myelin protein zero (P0), and an increase in regulatory T cells. We conclude that S1P receptor modulators may play a therapeutic role in autoimmune neuropathies.

1. Introduction

Fingolimod (FTY720) is an oral S1P receptor modulator in phase III clinical trials for the treatment of multiple sclerosis (MS). A decrease in MRI and clinical disease activity was observed in a phase II study of FTY720 in MS (Kappos et al., 2006). FTY720 is highly efficacious in the MS model of experimental autoimmune encephalomyelitis (EAE) (Balatoni et al., 2007; Fujino et al., 2003; Webb et al., 2004). The beneficial effect of FTY720 in EAE is attributed to lymphocyte sequestration in secondary lymphoid organs, although it also enhances the expression of neuroregenerative genes in the CNS (Chiba et al., 1998; Foster et al., 2008; Graler and Goetzl, 2004; Mandala et al., 2002; Pinschewer et al., 2000). In addition, dynamic effects of FTY720 and related compounds in oligodendroglial lineage cells have been demonstrated (Coelho et al., 2007; Jaillard et al., 2005; Jung et al., 2007; Miron et al., 2008).

Not all treatments effective in MS also work consistently for autoimmune neuropathies such as chronic inflammatory demyelinating polyradiculoneuropathy (CIDP). For example, interferon beta (IFN-β) while effective in MS, has had contradictory outcome in CIDP (Hadden et al., 1999; Vallat et al., 2003). There is one report describing the beneficial effect of FTY720 (intraperitoneal injection) in P2-induced experimental allergic neuritis (EAN) in Lewis rats (Zhang et al., 2008). FTY720 is converted *in vivo* to FTY720-phosphate (FTY720P), which is a potent agonist of four of the five known S1P receptors (S1P1, S1P3, S1P4 and S1P5) (Brinkmann et al., 2002). It is unclear whether selective S1P1 modulators such as SEW2871 will have a similar therapeutic effect as FTY720 on EAN or EAE. T lymphocyte migration towards S1P gradient is highly dependent on S1P1 receptors, whereas dendritic cell migration is mediated primarily by S1P3 receptors (Allende et al., 2004; Maeda et al., 2007; Matloubian et al., 2004).

The goal of this study is to investigate whether FTY720 and selective S1P1 agonist SEW2871 exert a therapeutic effect in a model of spontaneous autoimmune polyneuropathy (SAP), the B7-2 knockout (KO) non-obese diabetic (NOD) mice. NOD mice are susceptible to the development of autoimmune diseases such as type 1 diabetes, thyroiditis, sialitis, or neuropathy, but disease manifestations are strongly influenced by co-stimulatory molecules and cytokine milieu (Salomon et al., 2001; Setoguchi et al., 2005). Elimination of a co-stimulatory molecule B7-2 in female NOD mice prevents type 1 diabetes and sialitis, but triggers the development of limb weakness at 6–7 mo, which progresses to quadriparesis by 8–9 mo. The incidence of neuropathy is lower in males compared to female B7-2 KO NOD mice. Unlike EAN, SAP mice do not undergo spontaneous recovery. Similar to human CIDP, electrophysiological findings in SAP are classical for a demyelinating process with superimposed axonal loss. Histological evaluation reveals the presence of inflammatory infiltrates ($CD4^+$, $CD8^+$ T cells, dendritic cells) in dorsal root ganglia and sciatic nerves but not in the CNS (Salomon et al., 2001). We and other investigators found that SAP is a Th1-mediated disease and that myelin protein zero (P0) is one of the autoantigens targeted by T cells

* Corresponding author. Dept. of Neurology MC2030, The University of Chicago, 5841 S. Maryland Ave, Chicago, IL 60637, United States. Tel.: +1 773 702 6393; fax: +1 773 9060.
E-mail address: bsoliven@neurology.bsd.uchicago.edu (B. Soliven).

0165-5728/$ – see front matter © 2009 Elsevier B.V. All rights reserved.
doi:10.1016/j.jneuroim.2009.07.006

in this model (Bour-Jordan et al., 2005; Kim et al., 2008; Louvet et al., 2009). In this study, we examined the effect of S1P receptor modulators on disease severity in SAP as determined by clinical assessment, electrophysiological, and histological evaluations. We also investigated the effect of these compounds at the level of the blood nerve barrier (BNB), on the autoreactivity to myelin P0, and on Schwann cell viability.

2. Materials and methods

2.1. Animals and reagents

All animal use procedures were conducted in strict accordance to the National Institutes of Health and University of Chicago institutional guidelines. Female B7-2 knockout (KO) NOD mice (7 mo old) were used for our studies. FTY720 (Novartis Pharma AG, Basel, Switzerland) was dissolved in distilled water. The drug was freshly prepared and given orally once daily by gavage at 0.3 to 1 mg/kg body weight. SEW2871 (Cayman chemical, MI, USA) was dissolved in dimethyl sulfoxide (DMSO) and diluted with water. SEW2871 was given orally twice a day by gavage at 10 mg/kg body weight.

2.2. Clinical and electrophysiology assessment

For clinical assessment, the following nominal scale was used: 0 – normal; 1 – flaccid tail; 2 – mild paraparesis; 3 – severe paraparesis; 4 – tetraparesis; 5 – death. Grip strength testing consisted of five separate measurements in each of two trials per session with a grip strength meter (Columbus Instruments, OH). Results of two trials were averaged for each mouse per session. After the last grip strength measurement, electrophysiologic studies of sciatic nerves were performed as described previously (Kim et al., 2008; Salomon et al., 2001). Briefly, recording needle electrodes were placed subcutaneously in the footpad. Right and left sciatic nerves were stimulated distally at the ankle and proximally at the sciatic notch using needle electrodes. Latencies, conduction velocities and peak to peak amplitudes were measured. Temperature was maintained at ≥30 °C during the recording. Values obtained from right and left sciatic nerves were averaged for each animal, which was then used to calculate mean ± SEM (n = number of animals).

2.3. Histological studies

Segments of the sciatic nerves were fixed in 0.5–4% paraformaldehyde, embedded in OCT compound, and snap frozen. Longitudinal sections (10 μm slices) of sciatic nerves were stained with hematoxylin–eosin (H&E), and inflammatory cells were counted at 20× magnification with tissue areas measured by image analysis. At least 3 sections were analyzed per nerve. For semithin/epon sections, nerve tissues were obtained at high sciatic levels prior to bifurcation, fixed in 4% PFA, postfixed in 1% osmium tetroxide for 1–2 h, embedded in plastic resin and stained with toluidine blue. The number of myelinated fibers over a total area of 0.09 mm^2 was counted with results expressed as % loss of myelinated fibers compared to unaffected nerves from preclinical mice. Sections were also scored using a semi-quantitative grading system: 0, normal; 1, < 25%; 2, 25–50%; 3, 51–75%; and 4 with > 75% demyelinated or thinly myelinated fibers. All histological analysis was performed in a blinded fashion.

2.4. Blood nerve barrier permeability

Evans blue albumin (EBA) solution was prepared as a mixture of 5% bovine albumin (Sigma, MO, USA) and 1% Evans blue dye (Sigma, MO, USA) in distilled water that was filtered in a PD-10 desalting column (GE healthcare, NJ, USA). B7-2 KO NOD mice were given FTY720, SEW2871 or PBS via tail vein injection. Six hours post-injection, anesthetized mice were infused with 100 μl of EBA solution through the tail vein. After 30 min, sciatic nerves were harvested and snap frozen. Longitudinal sections (10 μm) of sciatic nerves were placed on microscope slides with coverslips mounted using 50% glycerin in water. Sections were visualized using a fluorescence microscope at 10× magnification. Integrated fluorescence intensity was analyzed using the NIH Image J program. For each nerve, at least 2 areas/section for 3 sections were examined.

2.5. Splenocyte culture, proliferation and cytokine production assays

For proliferation assay, splenocytes were cultured at a density of 5×10^5 cells/well in HL-1™ medium plus non-essential amino acids (Biowhittaker), L-glutamine (2 mM), sodium pyruvate (1 mM) and β-mercaptopurine (55 μM) in flat-bottom 96 well plates, then cells were stimulated with OVA peptide (20 μg/ml), P0 peptide (20 μg/ml) or P2 peptide (20 μg/ml). On day 3, these cultures were added for 16 h with 1 μCi methyl-[^{3}H] thymidine. A stimulation index was defined by cpm in the presence of antigen divided by cpm in the absence of the antigen. Supernatants collected at 48 h from replicate cultures were assayed for IFN-γ (Endogen, Rockford, IL), IL-2, IL-10 (BD Biosciences, San Diego, CA) and IL-17 (eBioscience, San Diego, CA) using ELISA Minikits. The following peptides were used as antigens: 1) P0 (180–199) (SSKRGRQTPVLYAMLDHSRS); 2) P2 (53–78) (TESPFKNTEISFKLGQEFEETTADNR); 3) OVA (323–339) (ISQAVHAAHAEINEAGR) (GenScript Corporation, Piscataway, NJ).

2.6. Schwann cell (SC) culture and cell viability assay

Primary SCs were prepared from P3–4 rats as previously described (Iwase et al., 2005; Nagano et al., 2001). After treatment with 10 μM cytosine arabinoside (Ara C) for 48 h to eliminate proliferating fibroblasts, SCs on polylysine-coated dishes were incubated with proliferating medium: DMEM containing 10% FBS, 2 μM forskolin (fsk) and 20 μg/ml bovine pituitary extract (BPE). SCs in passages 2 and 3 were used for experiments, after removal of fsk and BPE from culture medium for at least 3 days prior to experiments. For phosphorylation studies, SCs were incubated in serum-free medium (SFM) plus insulin (5 μg/ml), transferrin (5 μg/ml) and selenium (5 ng/ml) for 24 h prior to exposure to FTY720P for 15 min. For cell viability studies, trypan blue exclusion test was used to evaluate cell death upon serum withdrawal for 3 d in the presence or absence of test agents. Detached SCs (pre and post-trypsin treatment) were centrifuged, resuspended in PBS, stained with 0.4% trypan blue and counted using a hematocytometer.

2.7. Real-time PCR

The total RNA was isolated using a Trizol reagent (Invitrogen), followed by Qiagen column purification. Real-time PCR studies were performed as described previously (Jung et al., 2007). The following primers were used: S1P1-forward (5′-CTGACCTTCCGCAAGAACATCT-3′) and reverse (5′-CTTCAGCAAGGCCAGAGACTTC-3′); S1P2-forward (5′-ACATTTCTGGAGGGCAACAC-3′) and reverse (5′-TGGTCCCCA CAGTCACAGTA-3′); S1P3-forward (5′-AGAACGAGAGCCTGTTTCCA-3′) and reverse (5′-CAG CTTCCCCACGTAATCAT-3′); S1P4-forward (5′-GGACTTCGAGGTCACTCAGC-3′) and reverse (5′-CTGCCAAACATTCATCATGG-3′); S1P5-forward (5′-CTCTAGAGCGCCACCTTACCA-3′) and reverse (5′-CCCAGCAGCAGCGACAA-3′); GAPDH-forward (5′-TTC ACCACCATGGAGAAGGC-3′) and reverse (5′-GGCATGGACTGTGGTCATGA-3′).

2.8. Western blot analysis

Cell lysis, protein count, SDS PAGE and Western blot analysis were performed as described previously (Iwase et al., 2005; Jung et al., 2007). Sample proteins (30 μg per lane) were resolved by 15% Tris–

HCl gel electrophoresis (BIO-RAD, CA, USA) and blotted to polyvinylidene difluoride membranes (Millipore, MA, USA). The following primary antibodies were used in this study; anti-pERK1/2 (1:500), anti-pAkt (1:500), anti-ERK2 (1:500) and anti-Akt (1:500). All experiments were repeated at least three times with similar results. Representative data are shown. Results are expressed as percentage of control values by normalization of relative density of pERK1/2/total ERK2, and pAkt/total Akt to those from untreated conditions of each experiment.

2.9. Statistical analysis

Clinical and demyelination scores were analyzed by nonparametric methods Kruskal–Wallis or Mann–Whitney tests, as specified in the text or figure legends. Results from grip strength measurement, quantitative histologic analysis, and electrophysiology are expressed as mean ± SEM. Unless otherwise specified, statistical significance was determined by analysis of variance (ANOVA) followed by Student's *t* test and the Bonferroni method for multiple group experiments.

3. Results

3.1. Effect of FTY720 on disease severity in SAP

To examine possible therapeutic effects of FTY720 in SAP, animals were treated with FTY720 (0.3 mg/kg) ($n=5$), FTY720 (1 mg/kg) ($n=10$) or water (control, $n=11$) orally once daily at 7 mo of age (anticipated disease onset) for 4 weeks. At 7 mo (before treatment), there was no difference in median clinical scores amongst 3 groups. As shown in Fig. 1A, animals treated with water or FTY720 (0.3 mg/kg) exhibited worsening of clinical scores at 8 mo. By comparison, disease progression was significantly inhibited in animals treated with FTY720 (1 mg/kg), which was also reflected in grip strength measurements (Fig. 1B). Subsequent analysis was focused only in the FTY720 (1 mg/kg) group.

Electrophysiology and histologic studies were performed in a subset of study animals at 8 mo. Our previous studies in SAP mice (7–8 mo old) revealed that sciatic motor responses had prolonged distal latencies, slowed conduction velocities, and decreased amplitudes compared to those recorded from age-matched wild type NOD mice (Salomon et al., 2001). These observations were confirmed in this study. Distal latency was 3.1 ± 0.5 ms; conduction velocity was 15.5 ± 3.3 m/s; and amplitude was 1.46 ± 0.36 mV in untreated 7 mo old SAP mice ($n=8$). Values obtained from the water-treated group at 8 mo were similar to those recorded from untreated mice. As shown in Fig. 1C and D, there was a significant improvement in the distal latency and conduction velocity but not in the amplitude of the motor response in the FTY720 (1 mg/kg) group ($n=7$) compared to water-treated group ($n=6$).

Histological analysis by a blinded observer revealed a milder loss of myelinated fibers and lesser degree of demyelination in epon sections from FTY720-treated mice compared to those from water-treated group (Fig. 2A). The total number of myelinated axons/mm^2 was 10,533 ± 1992 in sections from water-treated mice, and 14,996 ± 1663 in sections from FTY720-treated group. Compared to unaffected nerves from preclinical mice, there was a 40.8 ± 12.8% ($n=6$) decrease in myelinated fibers in water-treated mice, and 10 ± 4.7% ($n=7$) decrease in FTY720-treated group ($p< 0.015$ by *t* test). In addition to the loss of myelinated axons, there were more demyelinated or thinly myelinated fibers in water-treated ones compared to FTY720-treated group. The median demyelination score was 2 for water vs 0.5 for FTY720 ($p<0.0.014$ by Mann–Whitney test). H & E staining revealed that there was a decrease in the extent of inflammatory infiltrates in nerve sections from FTY720-treated

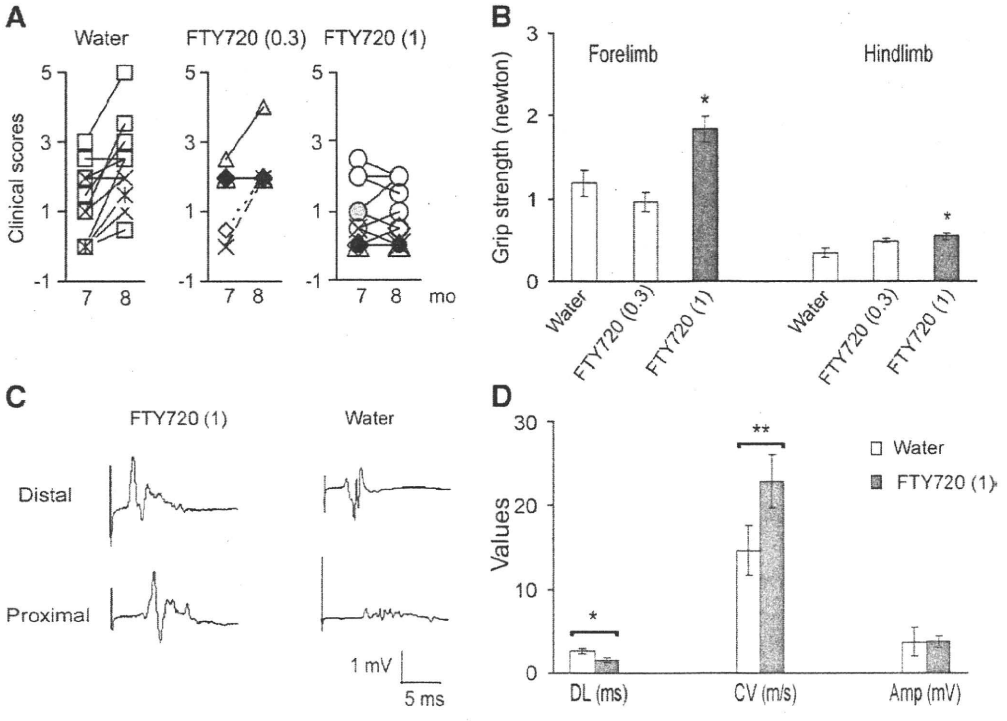

Fig. 1. Suppression of SAP in B7-2 deficient NOD mice by FTY720. Animals were divided into 3 groups: (1) water ($n=11$); (2) FTY720 at 0.3 mg/kg ($n=5$); and (3) FTY720 at 1.0 mg/kg ($n=10$). Daily oral administration was initiated at 7 months of age and continued for 4 weeks. A. Clinical scores. The median clinical score at 8 mo was 2.5 for water-treated group, 2.0 for FTY720 (0.3 mg/kg) and 0.75 for FTY720 (1 mg/kg); *$p< 0.0006$ for FTY720 (1 mg/kg) vs water (Mann–Whitney test). B. Hindlimb and forelimb grip strength measurements. *$p< 0.01$ for FTY720 (1 mg/kg) vs water. C, D. Examples and summary of sciatic nerve electrophysiology. Distal latency (DL), conduction velocity (CV), and amplitude (Amp) of sciatic compound muscle action potentials (CMAPs) were measured [$n=7$ mice for FTY720 (1 mg/kg) group, and $n=6$ for water-treated ones; *$p< 0.02$; **$p< 0.01$]. Subsequent analysis was carried out in FTY720 (1 mg/kg) group only.

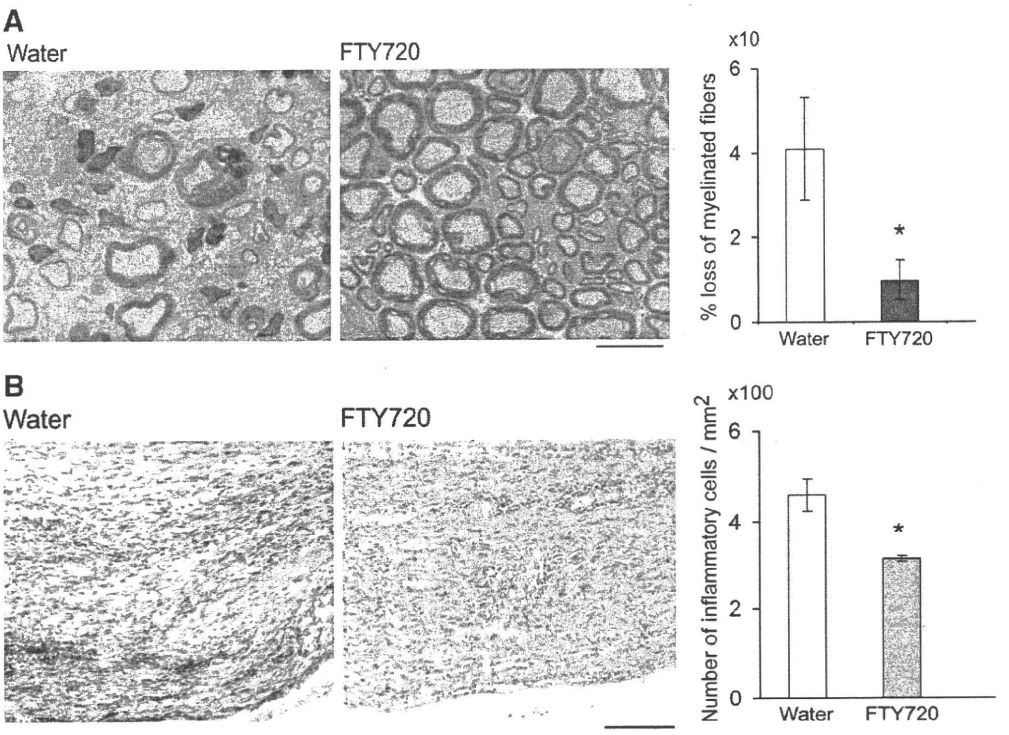

Fig. 2. FTY720 attenuates the severity of sciatic nerve pathology in SAP mice. A. Examples of epon sections from sciatic nerves of SAP mice treated with water or FTY720. Loss of myelinated fibers was attenuated in FTY720-treated mice compared to water-treated mice (*$p < 0.015$). Scale bar represents 20 μm. B. Examples of H &E sections of sciatic nerves showing decreased inflammatory cell infiltrates in FTY720-treated animals compared to water-treated ones (*$p < 0.02$). Scale bar represents 100 μm. For A and B, $n = 7$ for FTY720 group and $n = 6$ for the water group.

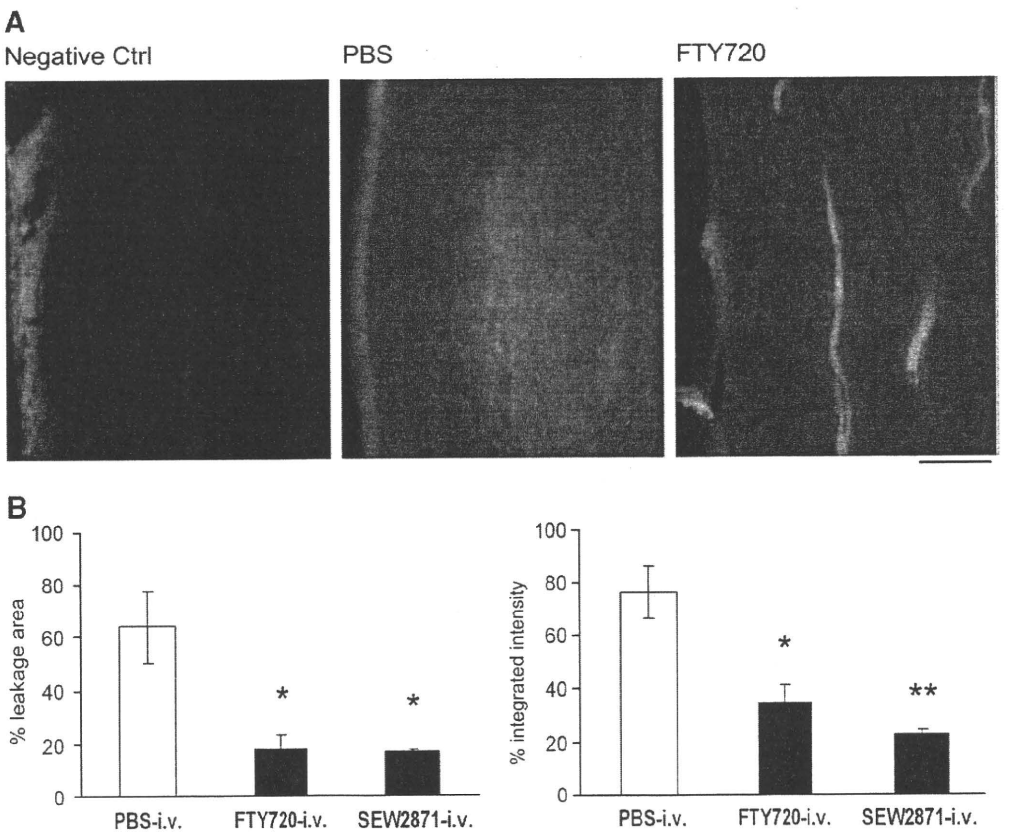

Fig. 3. Inhibition of blood nerve barrier (BNB) permeability by FTY720 in SAP mice. A. Examples of nerve sections from mice given Evans blue albumin (i.v.) 6 h after a single dose of intravenous FTY720, SEW2871 or PBS. Animals were sacrificed 30 min after Evans blue. Scale bar represents 100 μm. B. Data summary ($n = 3$ each). * For % leakage area, $p < 0.02$ for PBS vs FTY720 or SEW2871; for % integrated intensity, *$p < 0.02$ for PBS vs FTY720, **$p < 0.005$ for PBS vs SEW2871.

group compared to sections from water-treated ones, as shown in Fig. 2B. Thus, clinical, electrophysiological and histologic findings indicate that FTY720 treatment ameliorates the severity of SAP.

3.2. Mechanisms of action of FTY720 and SEW2871 in SAP

3.2.1. Effect on the blood nerve barrier (BNB)

Both functional S1P1 agonism on endothelial cells and functional antagonism at lymphocyte S1P1 receptors play a role in the attenuation of lymphocyte infiltration into target organs (Brinkmann, 2007). We investigated whether a single injection of FTY720 could prevent or attenuate the disruption of the BNB and whether a selective S1P1 agonist SEW2871 could mimic the effect. Sciatic nerve sections of PBS-treated mice showed leakage of EBA from microvessels into the surrounding endoneurium and perineurium; whereas the fluorescence of EBA remained within endoneurial microvessels in nerve sections from FTY720 and SEW2871-treated mice (Fig. 3A, B). These data indicate that S1P receptor modulators rapidly inhibit the disruption of the BNB via S1P1 on endothelial cells.

Given the above findings, we examined whether SEW2871 could also ameliorate the clinical severity of SAP. B7-2 KO NOD mice at 7 mo of age were administered SEW2871 or 4% DMSO (control) by oral gavage for 4 weeks. At 8 mo, clinical scores worsened in the DMSO group ($n=7$), but not in SEW2871-treated mice ($n=8$) (Fig. 4A). There was no decline in grip strength in SEW2871-treated animals, in contrast to that observed in DMSO-treated mice (Fig. 4B). Furthermore, sciatic nerve conduction studies revealed a significant difference in distal latency, conduction velocity and amplitude of the motor response in SEW2871-treated mice compared with control mice (Fig. 4C).

3.2.2. Effect on autoreactivity to myelin P0

We have recently reported that myelin P0 is one of the autoantigens in SAP, which is Th1-mediated (Kim et al., 2008). We examined the proliferative and cytokine responses of splenocytes isolated from control, FTY720- or SEW2871-gavaged mice. Treatment with FTY720 or SEW2871 led to a decrease in the proliferative response of splenocytes to P0 (180–199) compared to those from control mice. There was no response to OVA (323–339) and P2 (53–78) in all mice (Fig. 5A). IL-2 and IFN-γ levels were also decreased in splenocyte supernatants from FTY720- or SEW2871-gavaged mice compared to control mice (Fig. 5B). No significant effect on IL-10 or IL-17 levels was noted ($n=3$–4, not shown). In contrast, exposure of cultured splenocytes for 48 h to FTY720P (10–100 nM) or SEW2871 (100 nM) did not alter Th1 cytokine responses to P0 (180–199) ($n=3$, not shown). Mice treated with FTY720 or SEW2871 had increased percentage of $CD4^+Foxp3^+$ T cells and $CD4^+CD25^+Foxp3^+$ T cells in spleens and lymph nodes (LNs) compared to vehicle-treated mice (Fig. 5C). These results suggest that S1P receptor modulators tilt the balance in favor of regulatory T cells (Tregs) than effector T cells in B7-2 KO NOD mice.

3.2.3. Potential trophic/protective effect on Schwann cells

Real-time PCR studies revealed that S1P receptors are expressed by neonatal rat SCs with a relative mRNA level of S1P3>S1P2-S1P1>S1P4=S1P5 (Fig. 6A). Given the above, we investigated whether the active form of FTY720 (FTY720P) would exert glioprotective action or promote glial regeneration that could be pertinent in SAP. Treatment of SCs for 3 days with FTY720P in differentiating medium (0.5% FBS + ITS + forskolin) had no effect on SC differentiation based on P0 protein levels ($n=3$, data not shown). When serum withdrawal was used to induce cell death, the percentage of trypan $blue^+$ cells was decreased by FTY720P treatment (Fig. 6B). Western blot analysis showed that exposure of rat SCs to FTY720P (15 min) stimulated the phosphorylation of ERK1/2 (2.8 fold, $n=5$) and Akt (1.6 fold, $n=6$) compared to controls (Fig. 6C). However, we could not detect a difference in apoptotic ($TUNEL^+$) cells in nerve sections from FTY720-treated mice compared to those from control mice, possibly due to low frequency of $TUNEL^+$ cells at this particular time point (8 mo) (not shown).

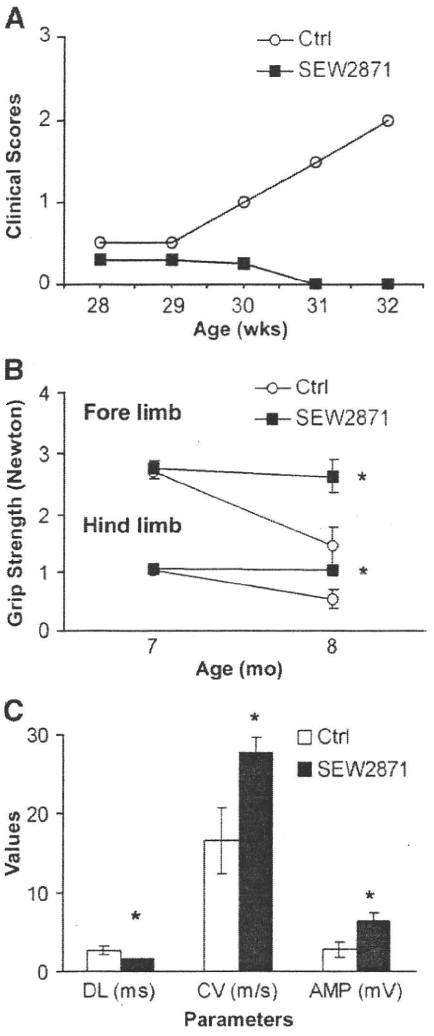

Fig. 4. Amelioration of SAP by SEW2871. SEW2871 (10 mg/kg) was given orally twice a day at 7 months of age and continued for 4 weeks. A. Median clinical scores ($n=7$ for Ctrl; $n=8$ for SEW2871). B. Grip strength measurements. * $p<0.007$ for SEW2871 vs Ctrl in forelimb at 8 mo, and $p<0.008$ in hindlimb. C. Data summary of electrophysiology at 8 mo ($n=6$ for Ctrl; $n=8$ for SEW2871). * $p<0.02$ for DL and CV; $p<0.03$ in Amp. In B and C, one vehicle-treated mouse died before grip strength measurements and electrophysiologic studies could be performed.

4. Discussion

FTY720, a prototype of S1P receptor modulators, acts acutely as an agonist at S1P receptors when phosphorylated to yield FTY720P, but preferentially desensitizes the $S1P_1$ receptor subtype upon prolonged exposure (functional antagonism). Not all lymphocyte subsets are affected equally. FTY720 induces a preferential depletion of naïve and central memory T cells but not effector memory T cells from the peripheral circulation of MS patients (Mehling et al., 2008). FTY720 also regulates B cell and dendritic cell migration (Cinamon et al., 2008; Lan et al., 2005). S1P1 activation induces an anti-inflammatory phenotype in macrophages and prevents monocyte-endothelial interactions (Hughes et al., 2008; Whetzel et al., 2006). These findings, taken together, suggest that therapeutic actions of FTY720